The Pennsylvania State University
The Graduate School
College of Health and Human Development

ENTROPY COMPENSATION IN HUMAN MOTOR ADAPTATION

A Thesis in
Kinesiology
by
Siang Lee Hong

Submitted in Partial Fulfillment
of the Requirements
for the Degree of

Doctor of Philosophy
August 2007

COMMITTEE PAGE

The thesis of Siang Lee Hong was reviewed and approved* by the following:

Karl M. Newell
Professor of Kinesiology
Thesis Adviser
Chair of Committee

Dagmar Sternad
Professor of Kinesiology

Joseph P. Cusumano
Professor of Engineering Science and Mechanics

John H. Challis
Associate Professor of Kinesiology
Director of the Graduate Program, Department of Kinesiology

*Signatures are on file in the Graduate School.

Abstract

Human movement is inherently variable, due to the number of controllable components that the motor system possesses and the relatively large number of potential movement patterns that can be employed to achieve a given goal. Motor variability has been known to be context-dependent, and thus, the structure of motor variability, as characterized by its probability distributions has been shown to change under different task and environmental constraints. This raises the possibility that the uncertainty or unpredictability contained within motor variability and at the level of the task and environment can be represented as entropies. This dissertation examined human motor adaptation to different task and environmental contexts with a view that this adaptive process can be represented as a process of entropy conservation through compensation. Three experiments were conducted to investigate the hypothesis that human motor adaptation reflects the process of entropy conservation. The first experiment examined the compensatory effects of spatial and temporal properties of visual feedback from the environment on the entropy of isometric force output. In this experiment, the entropy of the fluctuations of an index finger isometric force output under various levels of feedback frequencies (temporal) and visual gain (spatial). Increasing the entropy of the environment through reduced spatial and temporal information resulted in a decrease in the entropy of the force output, as indexed by a decrease Approximate Entropy (ApEn). This finding reflects a compensatory tradeoff between the effects of spatial and temporal entropy of the environment on the force output dynamics. Thus, at a constant level of task constraint, a decrease in entropy in the force output is noted when the entropy of the environment is increased. Experiments 2 and 3 were designed to examine the effects of

the task constraint on unimanual and bimanual isometric force production in conjunction with that of the environment. Here, the entropy of the environment was manipulated through feedback frequency, while the task entropy was altered via the ratio of the required force to the error tolerance. In Experiment 2, the entropy of the isometric force signal was measured with ApEn; in Experiment 3 the entropy of the motor output was assessed using the information entropy of the relative phase of the isometric forces generated by the index fingers of the left and right hand. As conservation processes are based on idealized cases, both entropy calculations were made conditional upon the probability of achieving the goal of the action, that is, remaining within the error tolerance bands. In both experiments, nonlinear decreases in the entropy of the force output were observed as the entropies of the task and environment were increased. Compensatory effects of the task and environmental entropies on the entropy of force dynamics were found, and these entropy tradeoffs were represented with a quadratic surface that captured a majority of the variance. These findings show that the context-dependent changes in motor variability in accordance with task and environmental contexts can be characterized through the compensation of entropy across the task, organism, and environment.

Table of Contents

List of Figures

List of Tables

Acknowledgements

My undying gratitude to my wonderful wife, Mollie, whose never-ending love and support has carried me through even the darkest of days. Much is also owed to my newly gained family for being their help at every step of the way. I am permanently indebted to my advisor, Karl Newell for providing me with an amazing experience as a graduate student, who has helped me gain the necessary tools for success in the future. Heartfelt thanks to the committee members: Dagmar Sternad, for many helpful conversations and advice; Joe Cusumano for many helpful insights that have shaped the conceptual framework of this dissertation; John Challis for providing me with the basic technical knowledge, and also helping me see the "lighter side" of science. My time here at Penn State has been enriched by being a part of a great lab, whose members, Eric James, Mei-Hua Lee, Rajiv Ranganathan, and Aileen Costigan for making this experience enjoyable on both a personal and professional level. Thanks also to the prior members of this lab, Kim Jordan, Jake Sosnoff, Paola Cesari, and Steve Morrison for being great friends with good advice. I must also extend many thanks to Peter Molenaar for his help on many conceptual and mathematical topics through numerous conversations that have aided immensely in the generation of this final product.

Chapter 1

Introduction

One of the most remarkable aspects of the human motor system is its ability to adjust its behavior to different task and environmental contexts. This adaptability comes from the many potentially superfluous *degrees of freedom* that the motor system possesses (Bernstein, 1967). Biological views of the motor system degrees of freedom most often describe them as the independent units controlled during action, for example, the individual joints, muscles, or motor units (smallest innervated pools of muscle fibers). With a vast resource of independently controllable movement units at its disposal, the motor system is endowed with the potential to generate a large pool of motor patterns to achieve a movement goal. This many-to-one mapping of movement patterns to a given goal is known as *motor redundancy*, where more than a single movement pattern can lead to the same task outcome (Arutyunyan, Gurfinkel, & Mirskii, 1969; Greene, 1969; Turvey, Fitch, & Tuller, 1982; Turvey, Shaw, & Mace, 1978).

These remarkably adaptive aspects of the motor system are conversely also the characteristics that pose the greatest challenges to understanding motor learning and control. This is due to the fact that generating a motor pattern requires some form of coordination in order to reduce the number of independent components of the motor system that must be controlled (Bernstein, 1967; Kugler, Kelso, & Turvey, 1980; Kugler & Turvey, 1987; Warren, 2006). However, even if the number of independent units to be controlled is reduced, redundant movement patterns are still available to the motor system, though not all of them will necessarily lead to the desired outcome, particularly if the context of the task and environment in which the movement is performed is altered.

These adaptable movement phenomena reflect the influence of the constraints on action (Kugler et al., 1980; Newell, 1986) that characterize human motor coordination as the product of the confluence of *organismic*, *task* and *environmental* constraints. The goal of this chapter is to seek to characterize categories of constraint, namely the organism, environment, and task using entropy as a common metric.

1.1. Probability and Entropy

Essentially, the basis for entropy is probability, and thus, Bernstein's view of human action as a process of selecting solutions to motor problems can be placed in terms of changes in *uncertainty* by the motor system as movements are being performed. These changes in the structure or probability distributions of variability thus lend themselves to an approach that is based around the concept of *entropy*. Shannon (1948) presented a form of entropy which was useful in characterizing the uncertainty contained within a signal passed across a communication channel that can be measured in binary units or "bits". Thus, uncertainty, H, can be calculated as:

$$H = -\sum_{i=1}^{n} p_i \log_2 p_i \quad \text{or} \quad H = \sum_{i=1}^{n} p_i \log_2 \frac{1}{p_i} \qquad (1.1)$$

This entropy is the sum across a total of n events, with p_i being the probability of the occurrence of the i^{th} event. In Figure 1.1, the method of calculating information entropy for three different probability distributions is presented. As in the bottom panel of Figure 1.1, when there is an equal probability of the occurrence of any event, i.e., all events are *equiprobable*, the entropy can simply be calculated as $-\log_2 p$ or $\log_2 (1/p)$. In the case of

data that are known to possess a Gaussian distribution, entropy can be derived from its variance, σ^2, and calculated as follows (see Shannon & Weaver, 1949):

$$H = \frac{1}{2}\log_2(2\pi\sigma^2 e) \qquad (1.2)$$

where, *e* is the Euler number, approximately 2.718.

A measure of sequential entropy (Beltrami, 1999) that is widely used in time-series analysis is Approximate Entropy (Pincus, 1991, Equation 1.3).

$$ApEn(\vec{X}, m, r) = \log\left[\frac{C_m(r)}{C_{m+1}(r)}\right] \qquad (1.3)$$

This measure provides an index of the unpredictability of future states from previous ones within a given time series $\vec{X}$, where C provides a count of the number of vectors of length *m* and *m* + 1 throughout $\vec{X}$ that are considered to repeat, as long as their difference falls within a tolerance range of *r*. Pincus (1991) showed that in regular/predictable time-series, values of $C_m(r)$ will be similar to $C_{m+1}(r)$, resulting in a ratio that is closer to 1, yielding ApEn values that are closer to zero. The base of the logarithm can be changed to 2 in order to obtain ApEn in bits. Lower ApEn values are thus indicative of a more regular time series, where similar patterns repeat and a lower amount of information is required to capture the dynamics of the fluctuations. Higher ApEn values are representative of an irregular time series, where the predictability of subsequent events or patterns in the data is low and is reflective of a higher amount of information content, a greater level of entropy within the sequence.

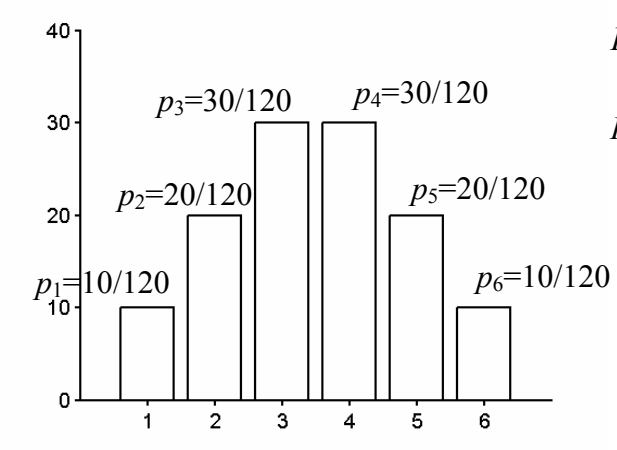

$$H = -\sum_{i=1}^{n} p_i \log_2 p_i$$

H =-[10/120 × $\log_2$ (10/20) +
20/120 × $\log_2$ (20/120) +
30/120 × $\log_2$ (30/120) +
30/120 × $\log_2$ (30/120) +
20/120 × $\log_2$ (20/120) +
10/120 × $\log_2$ (10/120)]
= **2.46** bits

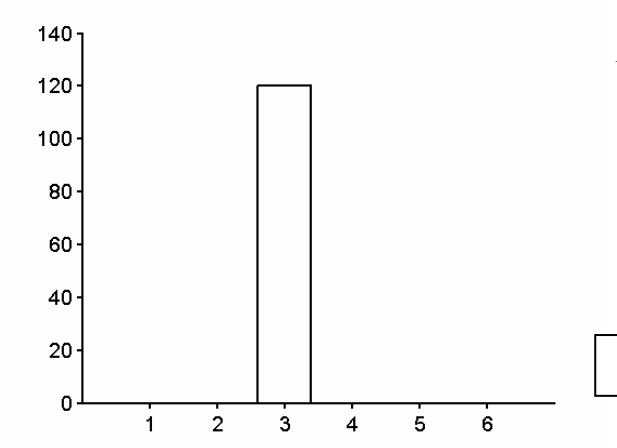

H =-[0 + 0 + 120/120 × $\log_2$ (120/120) + 0 + 0 + 0]
= 1 × 0
= **0.00** bits

No Uncertainty

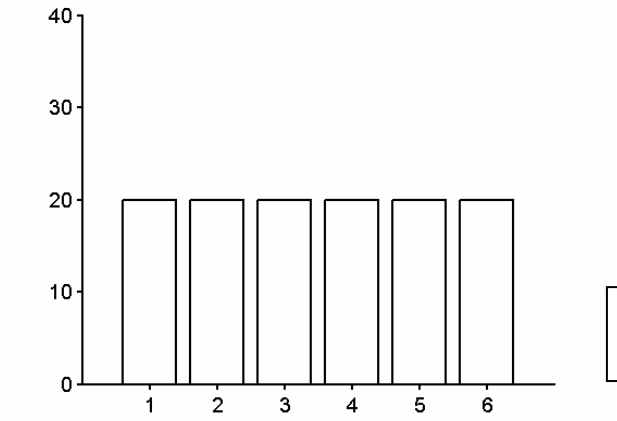

H =-[20/120 × $\log_2$ (20/120)
+20/120 × $\log_2$ (20/120)
+20/120 × $\log_2$ (20/120)
+20/120 × $\log_2$ (20/120)
+20/120 × $\log_2$ (20/120)
+20/120 × $\log_2$ (20/120)]
= - $\log_2$ (20/120)
= **2.59** bits

Maximum Uncertainty

Figure 1.1. Illustration of the calculation of information entropy for 6 possible outcomes for 120 data points. The middle and lower panels demonstrate the extreme cases of zero uncertainty and maximum entropy, respectively.

1.2. Entropy as a Description of Human Motor Variability

The probabilistic nature of human action is the basis for the study of the structure contained in motor variability, especially since it is now known that human motor variance often does not possess a Gaussian (normal) distribution and is also unlikely to be equally distributed (Newell, Deutsch, Sosnoff, & Mayer-Kress, 2006). The study of human action thus requires a conceptual framework that is focused primarily on probabilities, thus, making information theory a logical candidate for this framework as it provides a means of studying the probabilistic nature of human action. A primary reason of the use of information theory is that it provides a metric that allows the characterization of probability distributions.

Bernstein (1967, pp. 159-160) provided an early link between human motor variability and entropy, suggesting that the motor system's model of its future states is viewed as a table of probabilities of obtaining the desired movement outcome. Thus, Bernstein (1967) proposed that the present states of an action are constantly being compared with these probabilistic internal models of the future. The motor system then has to continually increase the probability of achieving the movement outcome until it reaches 1 (i.e., the goal is accomplished) by continually reducing the probability of undesired outcomes toward zero.

This raises the possibility that the structure of human motor variability can be captured through probability distributions and represented by a measure of entropy or uncertainty that changes under different task and environmental contexts. Entropy in the motor output, however, should not be viewed as a representation of the amount of control

being exerted upon the motor system, but rather, a high level of motor entropy is an indicator that a greater amount of information is necessary to describe the action.

1.3. Task and Environmental Entropy

Just as a probability-based approach can be used as a means of understanding the movement patterns of the actor, it can be extended to that of the task and environment. The information theoretic approach to experimental psychology has resulted in two long-standing views of human reaction time and movement time. The first, often termed *Hick's Law* or the *Hick-Hyman Law* (Hick, 1952; Hyman, 1953), relates the number of response choices within the stimulus display to the time required to initiate a response to the stimulus. *Fitts' Law* (Fitts, 1954; Fitts & Peterson, 1964) presented the speed-accuracy tradeoff in human aiming movements based on the ratio of the movement amplitude to target width. In the following section, we will return to the long-standing ideas of Hick's and Fitts' Laws in order to introduce evidence for redundancies at the level of the task and environment.

1.3.1. Environmental Entropy – Hick's Law

The human response to changes in the probabilities within the environment was characterized by Hick (1952) and Hyman (1953), demonstrating that the time taken to react to visual stimuli increases systematically with the number of choices presented. This is represented by a linear relationship between the logarithm of the number of S-R alternatives and reaction time (RT). In situations where n alternative stimuli occur with equal probability, at any given time, the probability, p, of the occurrence of any one of

the stimuli is 1/*n*. Thus, the entropy in these situations is equal to $\log_2 (1/p)$ or simply, $\log_2 (n)$. The formal usage of $\log_2$ is a means of transforming the S-R alternatives into binary units or bits of information, reflecting the number of "yes/no" options available to the individual responding to the stimuli. This relation between stimulus entropy and RT remains even when the probability of stimulus occurrence was no longer equal. Hyman (1953) demonstrated that RT remained linearly related to the entropy calculated from the weighted probabilities of stimulus occurrence even though the participants had no explicit knowledge that the stimuli would not occur with equal probability.

1.3.2. Task Entropy – Fitts' Law

Fitts (1954) presented the speed-accuracy tradeoff in human movement from the perspective of information theory. In order to understand increases in movement time with greater accuracy requirements, Fitts sought to frame the problem as one of information transmission in the motor system. For any given task, a movement with amplitude of *A* is required to move from the starting point to the center of the target. The maximum amount of error tolerance on either side of this center point is half the target width, *W*, and is thus, *W/2*. The probability of hitting the target is *W/2A*, which is the ratio of half the target width to that of the entire movement amplitude (Figure 1.2). It follows that a decrease in movement amplitude or increase in target width results in an increased probability of hitting the target. However, as previously noted (Equation and Figure 1.1), logarithms of fractions yield negative values, and entropy can be obtained from the logarithm of 1/*p*. In the Fitts (1954) context, *p* is equal to *W/2A*, and task entropy would thus be calculated as $\log_2 (2A/W)$. Fitts (1954) termed this logarithm of

the amplitude to target width ratio the *index of difficulty* (ID) and found that movement time increased linearly with ID. Fitts' Law in essence reflects that the amount of time taken to complete a movement is scaled to the task entropy.

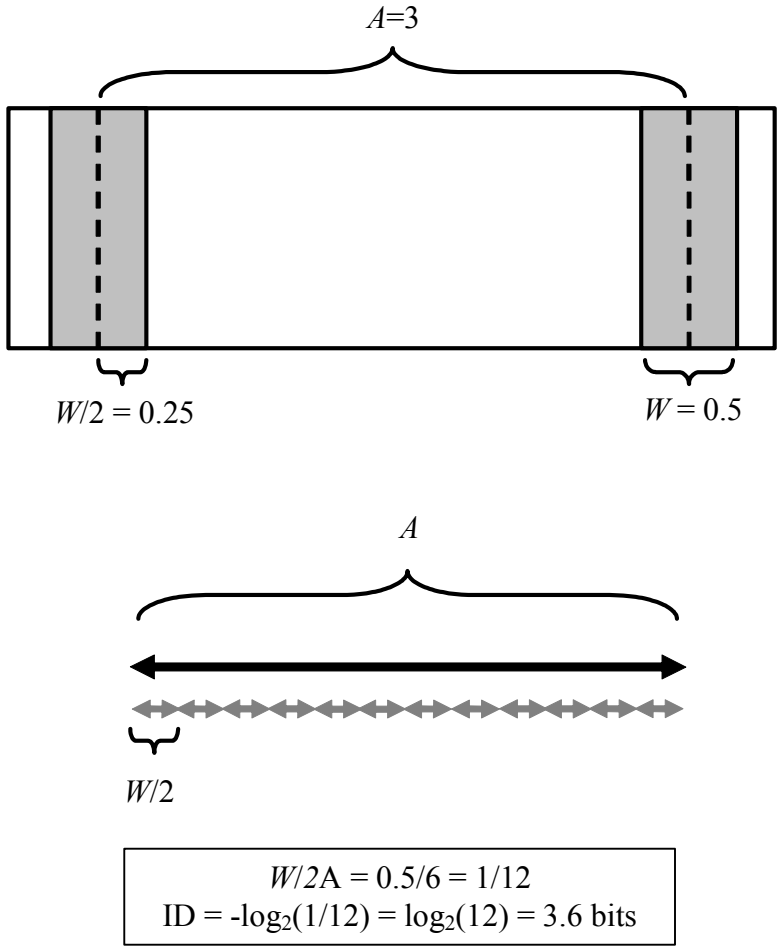

Figure 1.2. An illustration of the relationship between target width (W) and movement amplitude (A) in the derivation of the index of difficulty (ID). As the maximum allowable error on each side of the target center is $W/2$, and the probability, p, of striking the target is a ratio of maximum error to movement amplitude, yielding ($W/2A$). ID is meant to be equated to the information entropy, and is thus equal to log ($1/p$), hence ($2A/W$).

1.4. Organization of the Dissertation

With entropy as a common description of organism, environment, and task, the focus of this dissertation shifts toward the compensatory processes in human action encompassing the constraints of the task, organism, and environment. Working from the postulation that coordination is the product of the confluence of the task, organismic, and environmental constraints (Newell, 1986), this dissertation seeks to construct a view of human action as being reflective of a process of entropy conservation across the three categories of constraint. Based on the theorizing of Shaw and Turvey (1999), this dissertation will present a view of human motor adaptation as a process of entropy conservation, which is expected to be reflected by compensation or tradeoffs in entropy both within and between the various constraints.

In Chapter 2, the entropy conservation framework is constructed, with key examples of task-organism and environment-organism tradeoffs in entropy are provided. This gives rise to the postulation of the conservation of entropy. Chapter 3 contains Experiment 1, designed to test the hypothesis that the effects of spatial and temporal entropy of the environment on the entropy of motor output are compensatory. It is predicted that increasing the environmental entropy will result in a decrease in the sequential entropy of the isometric force dynamics.

Chapters 4 and 5 contain Experiments 2 and 3, which seek to extend the findings of Experiment 1 to include the entropy of the task. Using a unimanual isometric force task in Experiment 2, and a bimanual task in Experiment 3, these examined the hypothesis that the effects of task and environmental entropy on the entropy of the motor output are compensatory. Based on the postulation of conserved quantities in human

action (Shaw & Turvey, 1999), it is expected that increasing levels of the task and environmental entropies will result in a decrease in the entropy of the motor output. Lastly, Chapter 6 provides a general discussion across the experiments, highlighting limitations of the study along with directions for future research.

"*Alea iacta est*"

-- Julius Caesar

Chapter 2

Entropy Compensation across Task, Organism, and Environment

The production of a desired pattern of movement kinematics or kinetics is not usually the action goal itself as more than a single movement pattern is likely to achieve the desired movement goal (Bernstein, 1967). The review in Chapter 1 has led to a characterization of the task, organism, and environment using entropy as a common metric. As the environment provides information regarding the action that is being performed, the entropy of the environment is also dependent on the ability of the actor to obtain information from the environment. Similarly, task performance is dependent on the capacity of the motor system to achieve the necessary parameters of the task. As such, these sources of entropy interact, and their confluence guides the organization of human action (Newell, 1986).

As an intuitive and anectodal example of an interaction of constraints, when one attempts to walk across a dark room, the entropy in the environment is at its maximum, and thus, task entropy and organismic entropy must be reduced to compensate from this increase in environmental entropy. Generally, in this regard, smaller, more cautious steps are taken as a means of reducing the probability of bumping into a wall or stepping on an object. This reduction in movement amplitude is in keeping with Fitts' Law as a reduction in task entropy (see Chapter 1.3.2). At the motor level, the stiffer movements, where the joints are constrained through a change in muscle activation patterns in order to reduce entropy in the motor output.

In the other extreme case, if one intentionally walks with a stiff pattern in a normally illuminated room (a reduction in organismic entropy), the result will be an increase in entropy at the levels of the task and/or environmental entropy. At the level of the task, the likelihood of bumping into an object will be increased, as the likelihood of generating the right amplitude within a given precision region (target width) is decreased. As for the environment, the amount of attention that can be given to the objects and events occurring in the environment is decreased, thus, increasing environmental entropy. This change in the environment is similar to that of feedback frequency, as the actor is now unable to sample information from the environment as often as before. These intuitive examples raise the possibility that the interaction of the task, environmental, and organismic constraints can be characterized as tradeoffs in entropy between them.

In this chapter, the systematic and compensatory changes in entropy across the various categories of constraints will be explored, leading toward the proposal of entropy conservation within human movement.

2.1. Task-Organismic Entropy Tradeoffs

One example of the relationship between task and motor entropy is that of Harris and Wolpert (1998) who proposed a model of change in motor variance through the modulation of the magnitude of the motor command. In this model, the noise (random variation) surrounding the motor command is "signal-dependent" meaning that the magnitude of the noise increases linearly with the magnitude of the motor command. This concept holds common principles to the impulse-variability model of Schmidt,

Zelaznik, Hawkins, Frank, and Quinn (1979) where motor variability is a linear function of the impulse generated by the limb.

The Harris and Wolpert (1998) model was constructed to test the possibility that variance is a minimized quantity with respect to the task parameters. Harris and Wolpert (1998) sought to demonstrate that the findings in Fitts' Law were the result of the minimization of variance at the level of the motor output. The changes in movement time with increasing task entropy (as defined by the index of difficulty) through the minimization of motor variance. If the assumption of a Gaussian distribution is upheld, this finding could be viewed as tradeoff between task and organismic entropy, where increases in task entropy resulted in a reduction in motor entropy, knowing the relation between variance and entropy (see Equation 1.2).

Overall, these findings provide evidence for the proposition that organismic entropy is inversely related to task entropy. Movement goals that require task parameters that have a low probability of achievement (high task entropy) result in movements with lower entropy in their dynamics. Task parameters with a high probability of achievement (a task with low entropy) will allow for greater entropy in the action.

2.2. Environmental-Organismic Entropy Tradeoffs

Changing the availability of visual feedback from the environment leads to systematic changes in motor entropy. When participants are required to maintain a constant isometric force and are provided with their force trace on a computer monitor under differing feedback frequencies the entropy contained in their force traces is altered systematically (Slifkin, Vaillancourt, & Newell, 2000). An illustration of the

contributions that feedback frequency bring to a given force trace can be seen in Figure 2.1. From a no-intermittency condition (a continuous line) to approximately 10 Hz (10 dots/s) feedback frequency, there is no loss of performance (as indexed by the closeness of the force trace to the required line). As the frequency of feedback is decreased below 10 Hz, performance begins to degrade, as seen in increases in RMSE (root mean square error), which was provided to the participants as post-trial feedback. Using ApEn, developed in Pincus (1991), Slifkin et al. (2000) found that ApEn decreased systematically with increasing intermittency in the visual feedback. This reduction in ApEn can be equated with a decrease in entropy in the force output over the course of a trial. This effect of visual feedback intermittency has also been found in both constant level (Sosnoff & Newell, 2005a) and rhythmic/sinusoidal force production (Sosnoff & Newell, 2005b) tasks.

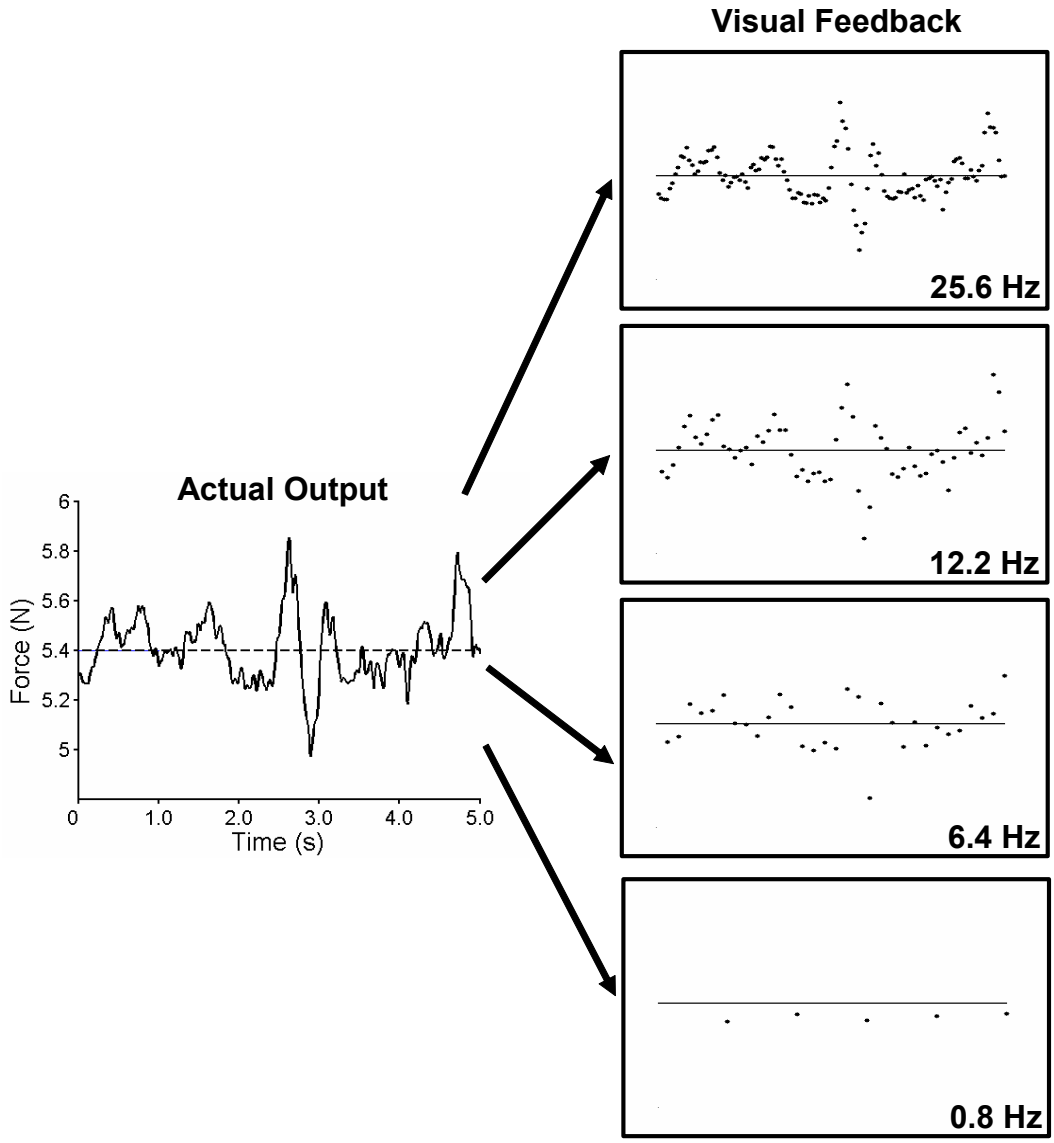

Figure 2.1. Illustration of feedback frequency from an actual force trace (left panel) at 25.6, 12.2, 6.4, and 0.8 Hz respectively (right panels). The right panels represent the actual visual feedback that a participant would be presented if the force trace on the left panel were generated.

Slifkin et al. (2000) found that providing feedback at a rate higher than approximately 6.4 Hz provided no further benefit to performance during a constant force production task. As the environmental entropy is decreased by the increasing feedback frequency (beyond the 6.4 Hz point), the information from the environment is increased.

This effect is similar to that of the task-organismic entropy tradeoff in Fitts' Law, as decreasing environmental entropy results in increases in ApEn of the force output. Beyond the breakpoint around 6.4 Hz, however, the participants' ability to match their force output to the desired level does not increase any further (see Figure 2.2). This finding is reflective of a decrease in motor entropy as the information from the environment is reduced.

The effect of visual feedback intermittency has also been found in two- and three-finger grip tasks. Sosnoff, Jordan, and Newell (2005) found similar effects of feedback intermittency on the ApEn of the grip force to that of the single finger. However, an extension to the previous findings was obtained from analyses of inter-digit individuation through Cross-Approximate Entropy, known as Cross-ApEn (Pincus & Singer, 1996), which provides a measure of the relative, sequential co-occurrence of data points of 2 time-series and is also a measure of mutual information or redundancy. From the grip task experiment, increasing feedback intermittency resulted in a decrease in Cross-ApEn that represents reduced independence of the fingers involved in the task, and hence greater redundancy between them.

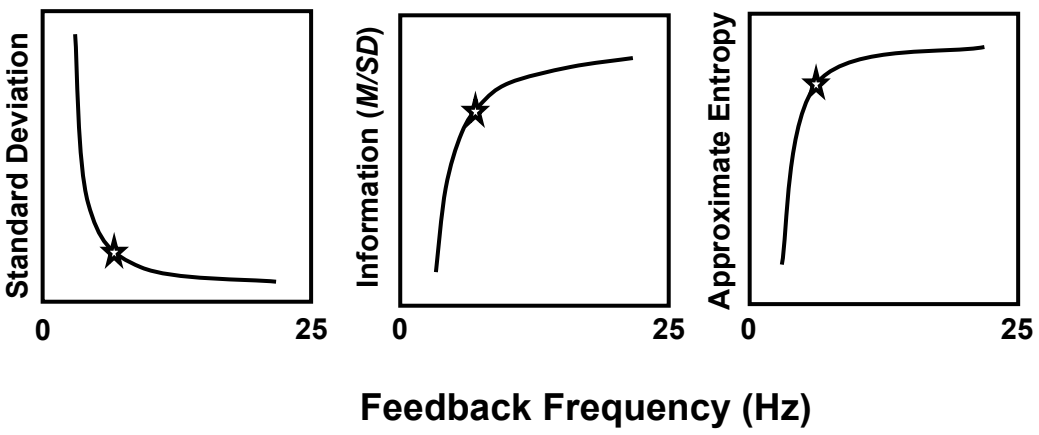

Figure 2.2. Schematic illustration of the effects of feedback frequency on the standard deviation, information, and Approximate Entropy (ApEn) of a force time series for the constant force production tasks. Approximate breakpoint locations are marked by stars.

The effect of feedback frequency on Cross-ApEn can be viewed as being the result of the increased entropy in visual feedback leading to greater redundancy between the fingers, reducing the overall level of motor entropy. In this view, the reduction in information presented on the visual display is compensated for through reduced entropy at the level of the organism. Evidence for a tradeoff between environmental and organismic entropy has been found in single finger (Slifkin et al., 2000) and multi-finger (Sosnoff et al., 2005) tasks with breakpoints in motor entropy (ApEn) occurring at relatively similar feedback frequencies in both tasks.

Another example of this environment-organism tradeoff was shown by Cusumano and Cesari (2006) who demonstrated in a pistol aiming task that the availability of a laser pointing light as additional information within the environment affects the dynamics of the arm during the task. Cusumano and Cesari studied the effects of different arm postures and viewing conditions on the ability of participants to maintain the position of a

pistol on a target placed at a 10m distance. The participants were required to perform the task with: 1) the arm extended with a laser pointer, 2) the arm extended with no laser, and 3) the arm abducted (elbow flexed at 90°) with a laser pointer. When the laser pointer was available, shifting from the fully extended position to the abducted position resulted in an increase in error variance. But, in the fully extended arm position without the laser, the error variance is similar to that of the abducted joint configuration. This finding shows that an increased organismic constraint (arm configuration) has a similar effect to a reduction in environmental information, via the removal of the laser pointer. This is a representation of the equality of organismic and environmental entropy, demonstrating the compensatory effects of organismic and environmental entropy on task performance.

2.3. Entropy Conservation as a Framework for Motor Adaptation

The studies reviewed in the previous section point to the effects of increases in task and environmental entropy leading to decreases in entropy at the level of the organism. This results in more predictable movement dynamics that can be described by fewer bits of information. Seemingly, human action can be described by compensatory tradeoffs in entropy across the task, environment, and organism. Shaw and Turvey (1999) proposed the idea of conserved quantities in human action, where a particular variable is being continually redistributed across the dimensions of the action. Without any explicit "instruction" or knowledge of these laws, objects in motion obey these laws, and hence, examining human action from the standpoint of conserved quantities has a potentially large role to play in understanding human behavior (Shaw & Turvey, 1999).

Here, we propose that human motor adaptation can be viewed as a process of entropy conservation across task, organism, and environment is present in goal-directed human movements under the idealized situation where the desired action goal is always achieved. A central prediction from the conservation of entropy is that the effects of task and environmental entropy on organismic entropy will be compensatory. As a consequence, increases in task and environmental entropy result in more predictable movements (decreased organismic entropy) and vice versa. These changes are reflective of compensation in entropy across the categories of constraints, where increases in task and environmental entropy lead to decreases in entropy at organismic level.

It is proposed that the compensation of entropy across all of the three categories of constraint can be viewed as a conservative process. Using the conservation of energy as an example, where the sum of kinetic energy and potential energy remains constant, $KE + PE = k$, which can be rewritten as $KE = k - PE$. Similarly, the entropies of the task, organism, and environment as a summing to a constant value, k, that can be represented by the function, $H_{org} + H_{env} + H_{task} = k$. This function reflects that the effects of increasing task entropy on the movement dynamics are mediated by decreases in environmental entropy, and vice versa.

Beyond this general relation, however, the entropy of the organism is viewed as being bounded at two extremes. The first limit is on the maximum level of entropy of the motor system. This limit arises from the inherent physical properties of the motor system, the muscles, ligaments, and tendons that connect the many skeletal structures of the body. As a result, the human motor system is unable to behave in an entirely random fashion (Newell, Deutsch, Sosnoff, & Mayer-Kress, 2006), even when task and

environmental entropy are zero, as represented by the constant, k in the function. At the lower extreme, a minimum level of entropy will always exist in the motor system and cannot be eliminated entirely through the organismic constraints, and thus, its output can never be completely predictable (Newell et al., 2006). It is proposed that this is due to the energy losses during the conversion from one form of energy to another (e.g., chemical to mechanical) during the production of movement or the maintenance of postures (Kugler & Turvey, 1987).

Another issue that arises in the development of the descriptive function for the entropy conservation process is the inherent nonlinearities in the relation between environment, task, and organism. Slifkin et al. (2000) observed nonlinear increases in ApEn with feedback frequency. Similarly, nonlinearities have been noted in Fitts' Law (e.g., Hancock & Newell, 1985), and is apparent in Harris and Wolpert (1998) as well. Thus, the function that is used as a description of this conservative process should also account for these nonlinearities.

One of the simplest functions that is able to account for both the nonlinearities in the empirical data and the concepts presented in Newell et al. (2006) is a sum of quadratic functions, $z = k + x^2 + y^2$. A similar function has been used in Newell, Liu, and Mayer-Kress (2005) that describes motor learning as a process that occurs along two independent time scales. This function will be adopted in this dissertation as a description of the process of entropy conservation. In Newell et al. (2005) behavioral patterns or performance scores were depicted by the elevation of the landscape, z, while the time scales of change were represented by the horizontal dimensions of the surface, x and y. Learning was predicted to result in a point of best performance, as denoted by the

constant, *k*. For the purposes of this dissertation, the behavioral patterns and performance scores can be viewed as reflective of the output of the organism, but will now be assigned entropy as units. Newell et al. (2005) had also linked the time scales of learning to be reflections of generalized task constraints such as speed and accuracy, for example. The horizontal dimensions of the surface reflect independent and external constraints on the organism that will be used to represent the task, and environment in this dissertation, but placed within the common entropy metric presented in Chapter 1.

Hence, the effects of the task and environmental entropies on the organism will be represented by a function:

$$H_{org} = k - H_{env}^2 - H_{task}^2 \qquad (2.2)$$

where H_{org} represents the organismic entropy, and H_{task} and H_{env}, the entropy of the task and environment, respectively, with a constant, *k*. A surface generated from this sum of quadratic functions is presented in Figure 2.3. The effect of performing a task with 2.0 bits of entropy with the environmental entropy of 1.0 bits is similar to the performance of a task with 1.0 bits of entropy performed with the environmental entropy of 2.0 bits. As with the impact of the environment and task on the organism, a change in organismic entropy through intention, or practice and training will allow for the mediation of the effects of task and environmental entropy.

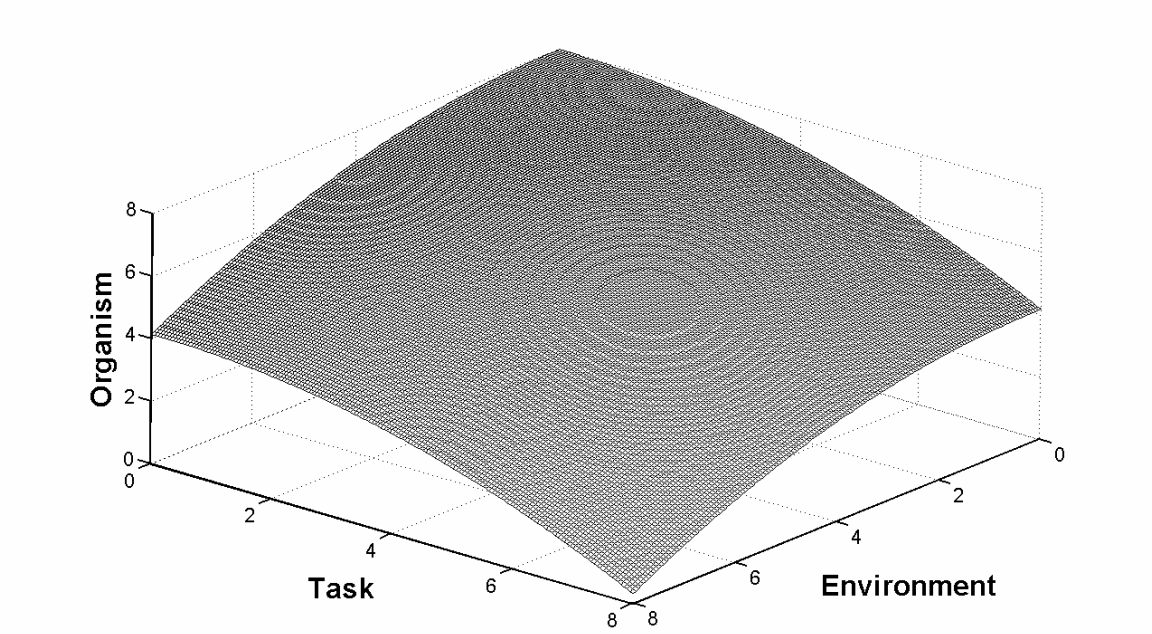

Figure 2.3. A 3-dimensional surface generated from the sums of 2 quadratic functions that converge to *k*, the shared intercept point: $H_{org} = k - H_{env}^2 - H_{task}^2$, where H_{org} is the organismic entropy, and H_{task} and H_{env} are the task and environmental entropies, respectively. The intercept, *k* would mark the maximal entropy that can be generated by the organism, creating the surface presented.

2.4. Summary

In this chapter, we have taken the concept of task, organismic, and environmental constraints on human action (Kugler et al., 1980; Newell, 1986) and presented their confluence as a process that is bound by a law of entropy conservation. A few key principles define this conceptual framework:

1. Entropy across the three categories of constraints, namely, the organism, task, and environment are compensatory and reflect its conservation. Increases in entropy at one category of constraint must be compensated by reductions in entropy of the other categories of constraints.

2. Human motor entropy is bounded at two extremes: i) a minimum level of entropy due to the inherent fluctuations in the organism itself; and ii) a maximum level where motor entropy is limited by the physical and neural linkages between the many components of the motor system.
3. This process of entropy conservation is the representation of an idealized case, where the movement goal is always achieved. Thus, as long as the ideal case is maintained, this process will be expected to hold true.

In summary, the entropy in human action is altered in a systematic and invariant pattern with that of the task and the environment in which it is being performed. This leads to a position that these systematic changes can be viewed as a natural law that conserves the entropy present at the three categories of constraints, namely, the task, organism, and environment.

Chapter 3

Compensatory Properties of Visual Feedback in Force Control

3.1. Abstract

This experiment investigated the hypothesis that spatial (gain) and temporal (frequency) properties of visual feedback on the control of isometric force output are compensatory. 12 participants performed an index finger isometric force production task with 5 different levels of visual gain and 4 feedback frequencies. There was a significant effect of gain on mean and standard deviation (SD) of the force output, while feedback frequency significantly affected the force SD and root-mean square error. Significant effects of gain and frequency and a gain × frequency interaction on the Approximate Entropy (ApEn) of the force, revealed the effect of visual feedback entropy on the force fluctuation dynamics. The combined effects of the spatial and temporal properties of visual feedback on ApEn were approximated by a sum of second-order polynomial functions, indicating their compensatory effect on the informational content of the dynamics of isometric force.

3.2. Introduction

Since Woodworth (1899) there has been continued interest in the role that visual information plays in the control of human motor performance (cf. Carlton, 1992; Desmurget & Grafton, 2000; Elliott, 1990). A classic paradigm is that of manual control in which "a person is receiving through his senses (visual, vestibular, tactile, etc.) information about the ideal states of some variables of a given system, as well as the output states of those variables, separately or in combination" (Sheridan & Ferrell, 1974, p. 171). In this theoretical and experimental framework, visual information is interpreted as reducing the entropy of the motor output in relation to the task goal as reflected in the tenets and indices of information theory (Fitts, 1954; Shannon, 1948). Such a reduction in entropy through the presence of visual information of force output can be manipulated by variations of the delay, gain, intermittency and frequency filtering of the force or movement output (Jagacinski & Flach, 2003)

One experimental test of information theory in manual control has been the manipulation of visual gain of the force output on the screen display (Stephens & Taylor, 1974; Newell & McDonald, 1994; Beuter, Haverkamp, Glass, & Carriere, 1995). Here it has been shown that enhancement of gain (pixel/Newton ratio; *p/N*) up to some level improves performance beyond which the performer cannot take advantage of the more precise information and may even lead to a performance decrement (Newell & McDonald, 1994). The findings from these studies suggest that there is an optimal level of gain for the experimental conditions that could be interpreted as an effect of visual angle, as the effects of visual gain on motor performance can be replicated by the distance from the computer monitor (Vaillancourt, Haibach, & Newell, 2006).

Sosnoff and Newell (2006) found the manipulation of gain to affect both the distributional and dynamic properties of isometric force output. A high number of *p/N* would mean that 1 N of force is presented over a larger area of the display, and thus, the feedback is more precise. Increasing visual gain resulted in higher standard deviations and coefficients of variation, leading to an increase in magnitude of variability. As a means of analyzing the properties of the force output dynamics, Detrended Fluctuation Analysis an alternative method of determining the self-similarity or fractal dimension (analogous to the spectral slope) of a non-stationary time-series was employed. This analysis revealed that greater visual gain did not necessarily lead to increased low amplitude, rapid fluctuations in force. Rather a U-shaped function emerged, where the middle gain level, approximately 128 *p/N*, resulted in the greatest amount of high-speed fluctuations. In an informational framework, these findings would suggest that the amount of information required to capture the fluctuations is greatest at the intermediate gain levels.

In a complementary intermittency paradigm of the frequency of visual feedback (Miall, 1996), Slifkin, Vaillancourt, and Newell (2000) found that decreasing visual feedback frequency (i.e., a reduction in the rate at which visual feedback is presented to the participants) led to an increase in magnitude of variability and a decreased ability to track the target force level in a constant isometric force production task, and thus greater error. This effect of visual feedback frequency has proven to be robust during different percentages of maximal force in the constant force task (Sosnoff & Newell, 2005a) and is upheld in rhythmic (sine-wave) isometric force production tasks (Sosnoff & Newell, 2005b). Across these studies (Slifkin et al., 2000; Sosnoff & Newell, 2005a, b), an

analysis of predictability within the force output fluctuations using Approximate Entropy (ApEn) revealed that decreasing feedback frequencies resulted in greater predictability within the force time series. In summary, the greater the amount of visual information provided within a unit of time leads to a high informational requirement for the description of the dynamics of the fluctuations in isometric force.

The studies of the effects of feedback frequency show that a greater amount of visual information in a smaller amount of time leads to more bits of information being required to describe the force output dynamics. Continually increasing the amount of space over which information is presented, however, does not lead to a similar result. Rather, it is possible that an optimal range is preferred by participants. Little, however, is understood regarding the combined effects of both the spatial and temporal properties of visual information on isometric force control as typically only one of the variables is normally manipulated with the other held constant at some apparently arbitrary parameter level.

It is relevant that in an analogy to the current problem, de Ruyter van Steveninck, Bialek, Potters, Carlson, and Lewen (1996) have found the spiking rate of the blowfly neuron responsible for motion detection to respond to both contrast and velocity of a visual display. By presenting a set of moving bars on a screen and altering the speed at which they moved side-to-side, as well as the contrast of these bars to the background, de Ruyter van Steveninck et al. (1996) were able to elicit different firing rates from the neuron. The result was a compensatory effect of velocity and contrast, where high levels of contrast with low velocity resulted in firing rates that were equivalent to that of high velocities with low background contrast. de Ruyter van Steveninck et al. (1996) then

employed a surface generated with a quadratic function as a means of capturing the relationship between spike rate and contrast and velocity. This function peaked at the highest levels of contrast and velocity, suggesting a convergence of functions of change in neuronal spike rate with contrast and velocity. This finding highlights the mutuality and complimentary nature of visual information sources in neuronal firing rates, which raises the possibility that mutual information is contained within the spatial and temporal properties of visual information used to control a motor output.

The goal of this study is to thus investigate the role of visual feedback manipulations on the informational content of muscle force output dynamics. Here, we systematically manipulate the gain and frequency of visual feedback as sources of spatial and temporal information. One of the main reasons of employing an isometric force production task is that the control of the force to the target level generated by the index finger cannot be guided by proprioceptive and tactile feedback alone (Sosnoff & Newell, 2005b). Realistically, the experimenter does not have direct control of the amount of information used by the participants for motor control. However, manipulations of gain and feedback frequency can be viewed as changes in the entropies in the spatial and temporal domain that can be obtained from the probability that no environmental information is available (Shannon, 1948). As such, entropies can be calculated based on the probability of occurrence from the limits of the visual system, and the display size. Based on the findings on the combined effects of velocity and contrast found by de Ruyter van Steveninck et al. (1996), it was hypothesized that spatial and temporal entropy will have similar compensatory effects on the informational content of the motor output.

3.3. Method

3.3.1. Participants

Twelve (6 female, and 6 male) right hand dominant (determined by preferred writing hand) adults between the ages of 19-33 years old (mean age of 23.8 years) participated in the study. All participants possessed normal or corrected-to-normal vision and no history of neuromuscular disorders. Informed consent was provided prior to participation, with approval for the experimental protocol from the Pennsylvania State University Institutional Review Board.

3.3.2. Apparatus

A 3-dimensional load cell (ATI Industrial Automation, Garner, North Carolina) was used to measure the force output. The normal force (*Fz*) force produced by the finger was the focus of the analyses as the task goal was to control this dimension of force. A schematic illustration of the experimental setup and the orientation of forces can be seen in Figure 3.1.

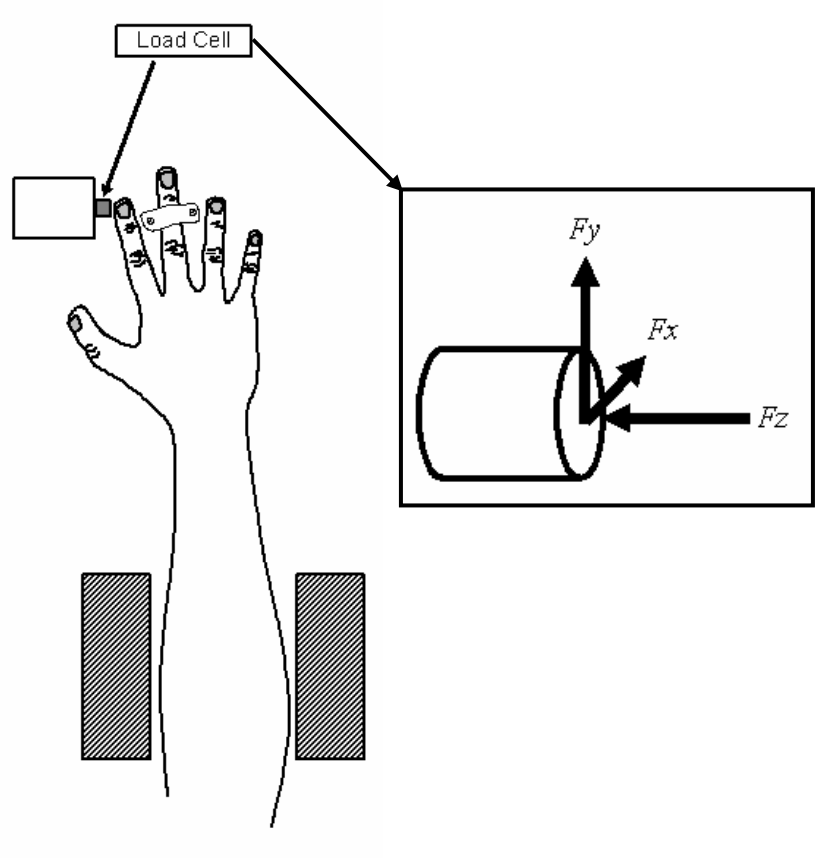

Figure 3.1. Schematic illustration of the experimental setup and load-cell orientation.

3.3.3. Procedures

MVC (maximal voluntary contraction) for each participant was determined at the beginning of the experimental session. Participants were instructed to exert maximal isometric force by pushing their index finger against the surface of the load cell as hard as possible. Force was generated by pushing against the load cell toward the midline of the body. Each participant completed 2 MVC trials of 10s with 20s rest between each trial. The average of the highest force value produced in each trial determined the respective MVC for each individual participant.

Following the determination of MVC, each participant was asked to match their force output to a red target line, which was 25% of their MVC, which appeared onscreen against a black background. The computer monitor on which the visual feedback was provided possessed a screen resolution of 800 (width) × 600 (height) pixels. Online feedback regarding their force output was provided via a force trajectory (plotted with white pixels) that passed from the left to right of the screen as the trial progressed. Upon completion of each trial, participants were provided with the RMSE (root mean square error) as post-trial feedback. RMSE was calculated as:

$$RMSE = \sqrt{\frac{\sum (F - f_i)^2}{(n-1)}} \tag{3.1}$$

where F is the target normal force value and f_i is the ith force sample in the time series.

Gain of the visual feedback was manipulated through the pixel/Newton (*p/N*) ratio, which altered the precision of visual feedback provided. 5 different gain conditions were employed with visual scales of 512, 256, 128, 32, and 2 *p/N*. These values correspond to the key conditions in Sosnoff and Newell (2006). Each of these gain levels were paired with 4 different visual feedback frequency conditions at 0.4, 3.2, 12.8, and 25.6 Hz (Slifkin et al., 2000), yielding a total of 20 independent conditions. The conditions were presented to the participants in random order and participants completed 3 blocked trials in each condition.

3.3.4. Data Analysis

Effects of the transitory forces at the beginning of the trial and the anticipation of trial termination were removed by omitting the initial 4 s and final second of each trial from the analysis. The cropped raw data were then filtered with a digital ninth-order Butterworth low-pass filter with a cutoff frequency of 30 Hz. From the cropped and filtered *Fz* force time series from each of the trials, mean, standard deviation (SD), and Approximate Entropy (ApEn) values were obtained. Root mean square error values were calculated for the normal force, *Fz* as a measure of the participants' performance, namely the ability to closely track the target force. Gain × Frequency (5 × 4) repeated measures ANOVAs were run independently on the 4 dependent variables using STATISTICA (Statsoft, Tulsa, OK). Where necessary, the Greenhouse-Geisser adjustment was applied to correct for any violations of the sphericity assumption.

ApEn was originally proposed as a measure of signal complexity or irregularity (cf. Pincus, 1991). The ApEn algorithm counts the relative recurrence of vectors of length m, $C_m(r)$, to that of vectors of length $m + 1$, $C_{m+1}(r)$, within a tolerance range of r, as presented in Equation 3.2. The final ApEn value is the natural logarithm of the ratio of $C_m(r)$ to $C_{m+1}(r)$. ApEn is also a measure of sequential entropy (Beltrami, 1999) and thus, in order to create a uniform informational metric, the base-2 logarithm is used to provide the ApEn values in bits. As recommended by Pincus (1991), the value of m was set at 2, while r was set to 0.2 of the standard deviation of the time-series.

$$ApEn(\vec{X}, m, r) = \log_2\left[\frac{C_m(r)}{C_{m+1}(r)}\right] \qquad (3.2)$$

Generally, in regular/predictable time series, values of $C_m(r)$ will be similar to $C_{m+1}(r)$. Thus, smaller values describe a more regular time series, where similar patterns follow

one another, and a low amount of information is required to capture the dynamics of the force fluctuations. Higher ApEn values are suggestive of an irregular time series, where the predictability of subsequent events or patterns in the data is low and is reflective of a higher amount of information content, a greater level of entropy in the motor output.

In order to convert gain and frequency into an information theoretic framework, *information entropy* or *entropy* measures were obtained from the *p/N* ratio and feedback frequencies. Information entropy (Shannon, 1948), *H*, is calculated as:

$$H = \log_2 \frac{1}{p} \tag{3.3}$$

where *p* is the probability of occurrence, assuming an all events or symbols have an equal likelihood of occurring. Here, visual gain is represented as *spatial entropy*, where increased gain provides more information and thus covers a larger portion of the computer monitor. The higher the gain level, the lower the spatial entropy. A display resolution of 800 × 600 pixels yields the possibility of 600 pixels available for the provision of visual information at any given point in time. The probability, *p*, can then be estimated as the ratio of gain in *p/N* to that of the total number of pixels available at a single point in time. Spatial entropy at each level of gain will then be $\log_2(600/Gain)$. The visual gain levels of 512, 256, 128, 32, and 2 *p/N* provide spatial entropy values of 0.2, 1.2, 2.2, 4.2, and 8.2 bits, respectively.

Frequency is represented as *temporal entropy*, as the feedback intermittencies result in gaps of different sizes between each presentation of the force output point on the display. As such, lower feedback frequencies result in greater temporal entropy. This entropy will be estimated based on the boundary conditions of the maximal capacity of the human eye. From Landis (1954), the positioning of the participants with respect to

the monitor will yield a critical Flicker-Fusion Threshold (FFT) of approximately 36 Hz, due to a 3º visual angle. The critical FFT is the frequency at which a flashing dot presented to participants becomes indistinguishable from a continuous, steady presentation. Therefore, temporal entropy was estimated as $\log_2(36/Frequency)$. The visual feedback frequencies of 0.4, 3.2, 12.8, and 25.6 Hz provide temporal entropy values of 6.5, 3.5, 1.5, and 0.5 bits, respectively.

3.4. Results

Repeated measures ANOVAs revealed significant main effects of visual feedback gain on the mean ($F(4, 132) = 4.78$, $p = 0.0027$) and SD ($F(4, 132) = 3.42$, $p = 0.0162$) of the force produced. The main effect of frequency was significant for the dependent variables of SD ($F(3, 132) = 12.78$, $p<0.0001$) and RMSE ($F(3, 132) = 23.93$, $p<0.0001$). For ApEn, both main effects of gain ($F(4, 132) = 9.15$, $p<0.0001$) and frequency ($F(3, 132) = 54.21$, $p<0.0001$) proved to be significant along with the gain × frequency interaction ($F(12, 132) = 3.33$, $p = 0.0003$). The *F*- and *p*-values for the main effects and interaction obtained from the statistical analyses are summarized in Table 3.1.

Table 3.1. Summary of results obtained from the repeated measures ANOVAs for the 4 dependent variables.

Dependent	Gain		Frequency		Gain x Frequency	
Variable	*F*	*p*	*F*	*p*	*F*	*p*
Mean	4.78	0.0027†	0.36	0.7848	0.54	0.8846
SD	3.42	0.0162*	12.78	<0.0001‡	1.75	0.0629
RMSE	1.52	0.2120	23.93	<0.0001‡	1.65	0.0848
ApEn	9.15	<0.0001‡	54.21	<0.0001‡	3.33	0.0003†

*$p<0.05$; †$p<0.01$; ‡$p<0.0001$

Tukey post-hoc comparisons of the levels of the main effect of gain on mean force revealed a significantly (p<0.05) lower mean force output for the lowest level of gain (2 *p/N*) when compared to all the other levels (Figure 3.2.A). A post-hoc analysis of the main effect of gain on SD, found significantly lower SD values at the highest gain level (512 *p/N*) when compared to the 2 lowest gain levels, namely 2 and 32 *p/N* (Figure 3.2.B). The upper panel in Figure 3.3.A shows the results of the Tukey post-hoc test on the main effect of visual feedback frequency on the SD of the force output. The post-hoc test found a significantly higher SD for the lowest feedback frequency (0.4 Hz) when compared to the other levels. Similar post-hoc test results were obtained for the main effect of frequency on RMSE (Figure 3.3B).

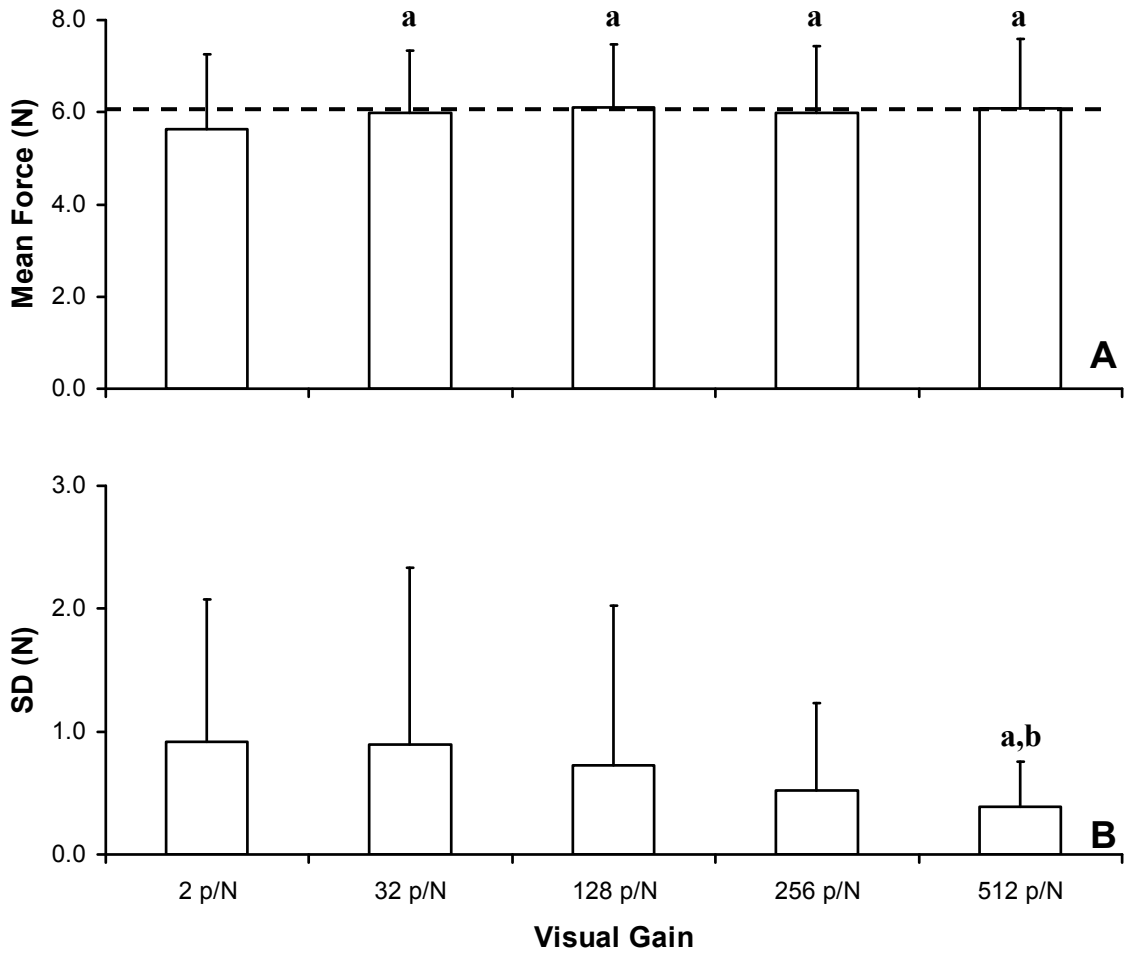

Figure 3.2. Mean (A) and SD (B) of the force output under different gain conditions. [a] and [b] indicate significant (p<0.05) difference from 2 *p/N* and 32 *p/N* respectively. The dashed line on the upper panel marks the between-subject average target force of 6.1 N.

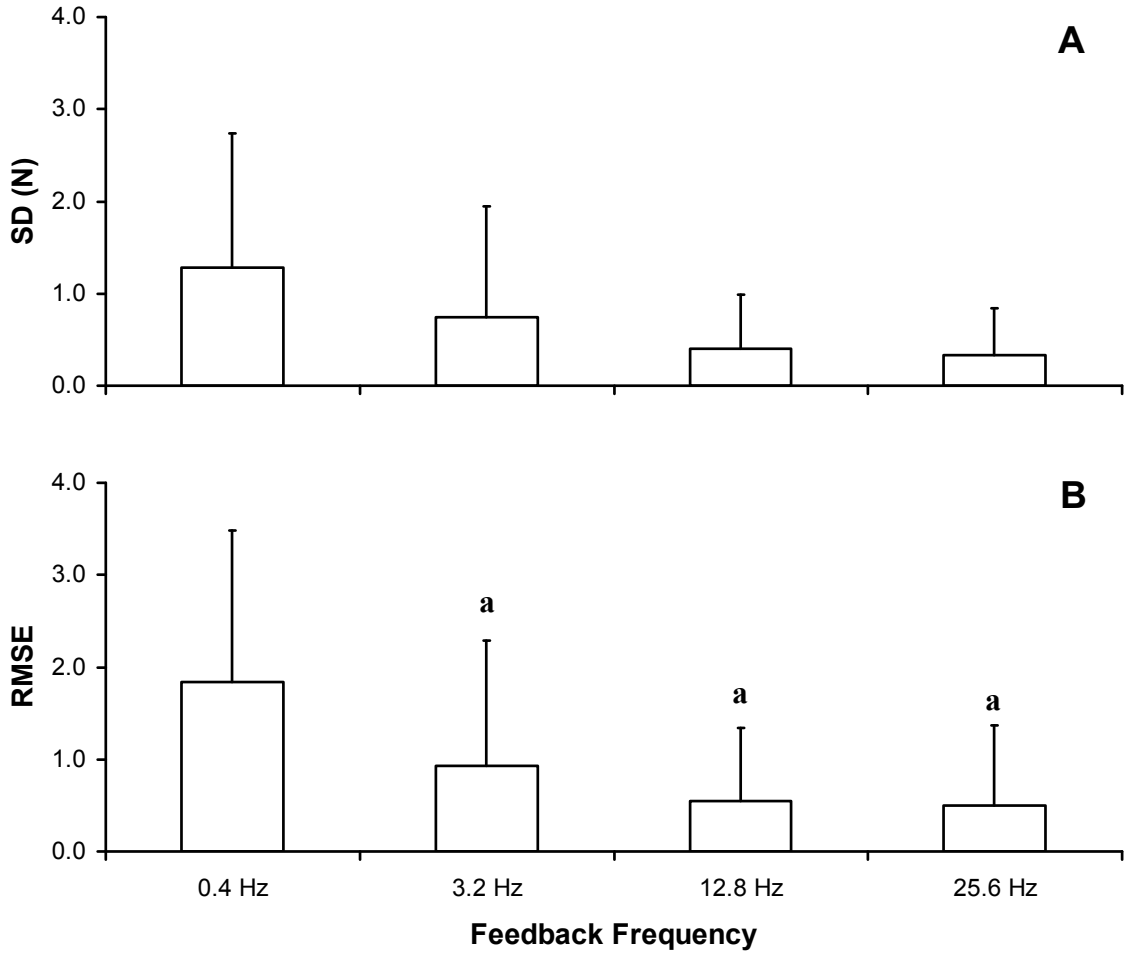

Figure 3.3. Force SD (A) and RMSE (B) with feedback frequency. [a] indicates significantly (p<0.05) different from 0.4 Hz.

The effect of visual gain on ApEn approximated an inverted-u shaped curve. As such, the Tukey post-hoc analysis did not find significant differences between the highest and lowest levels of visual gain. The Tukey post-hoc analysis of the main effect of frequency found that ApEn values differed significantly from one another with the exception of the two highest feedback frequencies, namely, 12.8 Hz and 25.6 Hz. The post-hoc results obtained for the significant main effects of gain and frequency on ApEn are presented in Table 3.2.

Table 3.2. *p*-values obtained from the Tukey post-hoc tests of the main effects of gain and frequency on ApEn.

Gain Level	2 p/N	32 p/N	128 p/N	256 p/N	512 p/N
2 p/N	---	0.0631	0.0022*	0.0057	0.9698
32 p/N	0.0631	---	0.7127	0.8853	0.0129*
128 p/N	0.0022*	0.7127	---	0.9971	0.0004
256 p/N	0.0057†	0.8853	0.9971	---	0.0010†
512 p/N	0.9698	0.0129*	0.0004†	0.0010†	---

Frequency Level	0.4 Hz	3.2 Hz	12.8 Hz	25.6 Hz
0.4 Hz	---	0.0002†	0.0002†	0.0002†
3.2 Hz	0.0002†	---	0.0203*	0.0034†
12.8 Hz	0.0002†	0.0203	---	0.8962
25.6 Hz	0.0002†	0.0034†	0.8962	---

*$p<.05$; †$p<.01$;

Representations of the gain × frequency interaction found for ApEn can be seen in Figure 3.4. The upper panel presents the effect of visual gain on ApEn at the different feedback frequencies, while the lower panel presents the effect of feedback frequencies of ApEn at the different levels of visual gain.

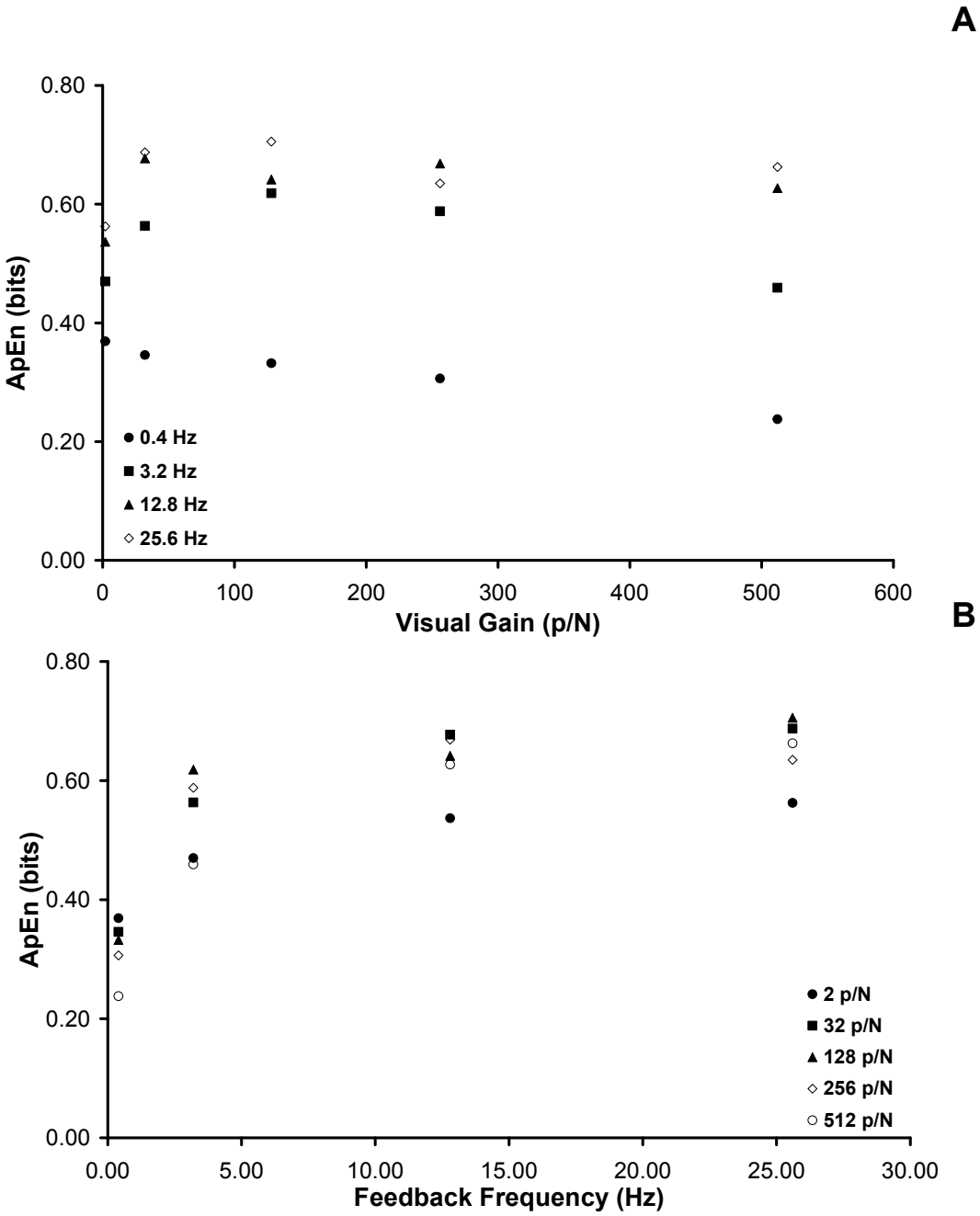

Figure 3.4. Effects of visual gain on force output irregularity (ApEn) separated by levels of frequency (A). Effects of feedback frequency on force output irregularity (ApEn) separated by levels of visual gain (B).

Visual gain and feedback frequency in the common informational metric of spatial and temporal entropy and their relation to ApEn are presented in 3.5.A and 3.5.B, respectively. With data from all the participants quadratic function fits yielded r^2-values of 0.85 and 0.90 for the spatial and temporal entropy, respectively. Following de Ruyter van Steveninck et al. (1996), a 3-dimensional surface was created to capture the interaction between spatial and temporal entropy on ApEn from the sums of the quadratic function fits. The intercept, xy_0, was obtained from an average of the intercepts of both the fitted functions. The final function for the surface can then be described in terms of spatial (x) and temporal (y) entropy:

$$ApEn = xy_0 - 0.0054x^2 + 0.04x - 0.0063y^2 - 0.01y \qquad (3.4)$$

The generated response surface is able to explain 69% of the total variance and is presented in Figure 3.5.C.

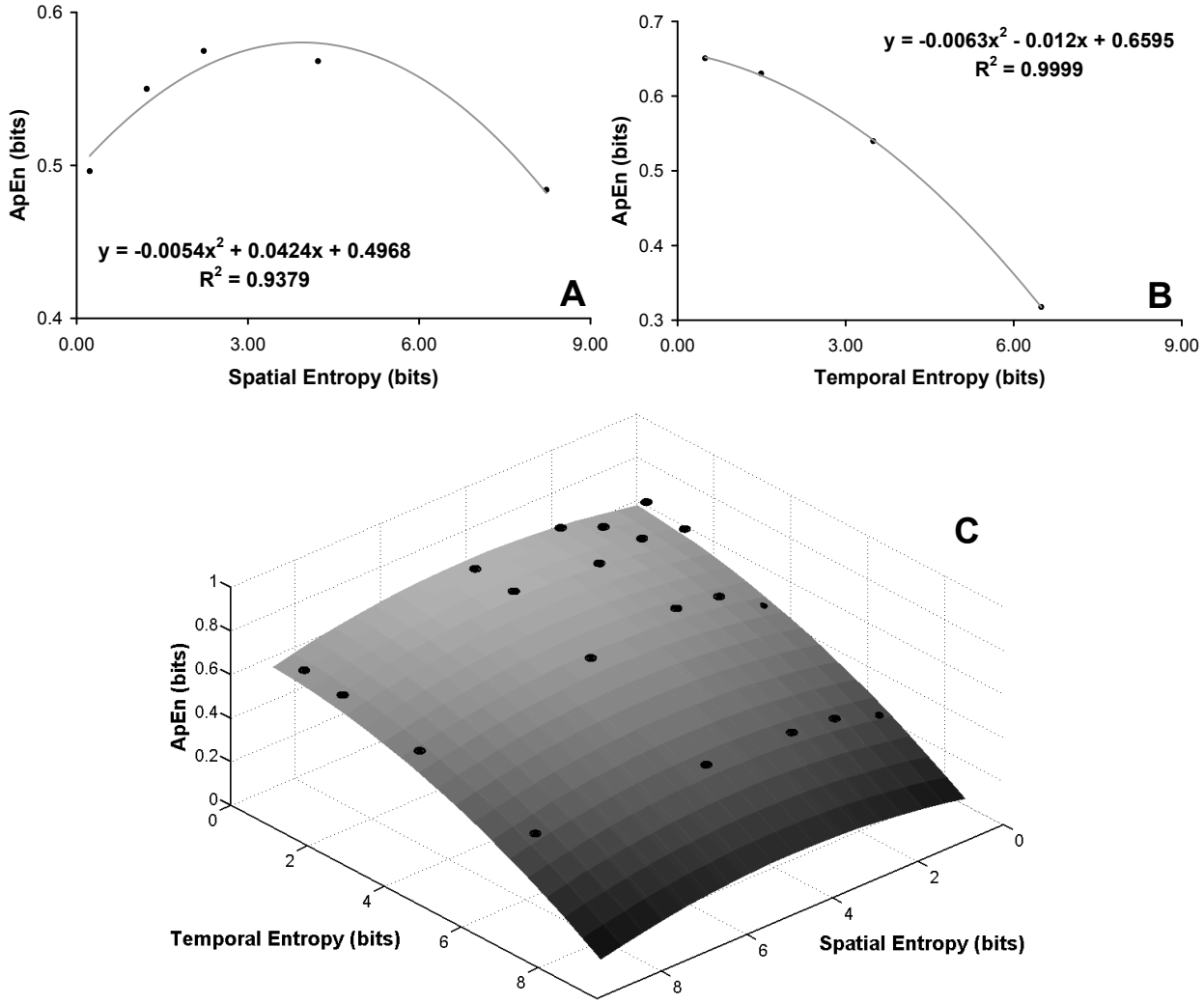

Figure 3.5. ApEn as a function of spatial (A) and temporal (B) entropy of the environment. The least-squares fitted functions (solid grey lines) and r^2-values are presented in each panel. Entropy surface obtained from the sums of the second-order polynomial function fits of ApEn to spatial and temporal entropy (C).

3.5. Discussion

The effects of visual gain and frequency of visual feedback significantly changed the amount and structure of variability in force output. Visual gain significantly affected the mean force produced, while feedback frequency significantly affected the magnitude and structure of variability. The central finding is the interaction between visual gain and frequency feedback revealed compensatory effects of spatial and temporal entropy in the visual display on the information needed to describe the force output dynamics.

3.5.1. Feedback Effects on the Distributional Properties of Force Output

Visual gain significantly affected the mean and SD of the force generated by the participants. The significantly lower mean force output at 2 *p/N*, the lowest visual gain, is suggestive of a tendency to undershoot the target when visual feedback is less sensitive to fluctuations in force produced by the finger. As gain increased, participants were able to generate forces that were closer to the target (see Figure 3.2). Magnitude of variability was significantly higher at lower gain levels, namely 2 and 32 *p/N* compared to the highest gain level of 512 *p/N*. Frequency of the visual feedback, however, had no effect on mean force produced. Magnitude of variability and variable error were both significantly affected by the frequency of visual feedback. At the lowest feedback frequency (2 Hz), SD and RMSE were significantly higher than all the other feedback frequencies.

What is clear from these findings is that magnitude of variability is reduced with increased feedback precision. As more feedback is presented within a smaller amount of time or space, the magnitude of variability is decreased. The ability to track the target

line over time, however, is dependent on feedback frequency, as indexed by the significant effect on RMSE. With a greater feedback frequency, participants were more able to make adjustments to deviations from the target line. Gain, however, affects the participants' ability to approximate the target line and produce the desired mean force. With low gain levels, the participants tended to undershoot the target, as a large undershoot would still be represented, spatially as being close to the line. Potentially, participants preferentially undershot the target as a means of reducing variability, knowing that the standard deviation of force has been found to grow exponentially with force output in such continuous force production tasks (Slifkin & Newell, 1999).

Another interesting finding is the change in between-participant variability with the feedback manipulations. From Figures 3.2 and 3.3, it is clear that there is an accompanying reduction in variability between participants as a function of feedback precision in both the spatial and temporal domains. These findings suggest that individual differences in motor performance are magnified by a reduction in visual feedback precision. This is in line with the study of the effect of visual gain on force output in older adults (Sosnoff & Newell, 2006).

3.5.2. Visual Information and the Dynamics of Force Output

When averaged across the different levels of feedback frequency, the amount of information required to capture the force output dynamics changed as an inverted-U function with increasing levels of gain (Newell & McDonald, 1994; Stephens & Taylor, 1974). Solving for the first derivative of the fitted quadratic function yields a maximum at 218 *p/N*, where the sequential entropy of the force dynamics is at its highest. This

finding is similar to that from Sosnoff and Newell (2006), where the scaling exponent of the Detrended Fluctuation Analysis was at its lowest between visual gain levels of 64 and 256 *p/N*. The effect of increments in feedback frequency resulted in a nonlinear decrease in the information contained within the force dynamics (see also Slifkin et al., 2000). Detailed inspection of the interaction between gain and frequency (Figure 3.4) shows that the function of change in ApEn was not similar across the different levels of frequency. At the lowest feedback frequency (4 Hz), increasing visual gain resulted in a decrease in motor information rather than the inverted-U shaped function. With different levels of gain, the general function of change with increasing feedback frequency is maintained, but differences in rate of change across the different gain conditions are apparent.

When the averaged data are converted to the entropy metric (Figure 3.5.A and 3.5.B), one can see that spatial entropy possesses an inverted-U relationship between ApEn, while increases in temporal entropy resulted in decreases in ApEn. When the effects of both entropies are combined through a sum of quadratic functions, the compensatory nature of the spatial and temporal properties of environmental entropy is made apparent. With the assumption that both functions converge toward a peak, the averaged intercept and the surface generated by the sum of the quadratic functions provides an explanation of the effects of entropy on the force output dynamics (Figure 3.5.C). This response surface represents the compensatory effects of spatial and temporal entropy on the entropy in the motor output, highlighting the mutuality inherent in spatial and temporal properties of the information in the environment. At the peak of the surface, spatial and temporal environmental entropies are at their lowest, and the entropy of the motor output dynamics is at its highest. Entropy of the motor output would be at

its lowest when both entropies are at their highest. The combined effect of entropy in the display occurs across the decreases in motor entropy as high levels of spatial entropy are compensated by low levels of temporal entropy and vice versa.

At low levels of entropy in the visual feedback display, greater entropy in the motor output is afforded. Greater levels of entropy in the visual display must be compensated for through an increase in predictability of the force fluctuations. At the lowest levels of visual display entropy, force output entropy reaches its peak. It is likely that such a limit to motor entropy is present due to musculoskeletal linkages that prevent the fluctuations in human postural tremor from being an entirely random (white-noise) process (Newell, Deutsch, Sosnoff, & Mayer-Kress, 2006). At the other extreme of the entropy scale, there is a maximum level of entropy in the visual feedback that allows for the task goal to be achieved. This is due to inherent entropy in the motor system that cannot be eliminated in its entirety (van Beers, Baraduc, & Wolpert, 2002). As such, a minimum amount of visual or haptic information from the environment would be requisite for the guidance of motor tasks. The most important finding, however, is that spatial information is able to compensate for a lack of temporal information and vice versa, an effect similar to the effect of velocity and contrast on the blowfly neuron (de Ruyter van Steveninck et al., 1996). Thus, situations where the precision of visual feedback in spatial terms is minimal, greater information presented within a shorter time window, and vice versa, may serve to reduce the entropy within the environment.

A lack of perfect symmetry of the response surface for spatial and temporal entropy, however, points to the problem that the entropies are not directly equivalent. Although this study has extended the findings of Sosnoff and Newell (2006) by using for

the size of the display as a means of estimating spatial entropy, temporal entropy can be, at best, approximated from assumptions based on physiological data. Potentially, the use of eye movement tracking technologies will aid in the understanding of the temporal properties in the acquisition of visual information.

Chapter 4

Entropy Compensation in Motor Adaptation

4.1. Abstract

This experiment tested the hypothesis that entropy is compensated across the changing constraints of the organism, task, and environment in human action. Participants generated an isometric finger force under different environmental (feedback frequencies) and task (force target width) constraints. Higher feedback frequency and narrower task tolerance range progressively decreased variability and the relation between the task constraint and force variability was nonlinear. Approximate Entropy, corrected for the probabilities of achieving the action goal, was represented by a quadratic surface that was lowered with increments of feedback frequency and task constraint. The findings provide initial evidence that motor adaptation to the confluence of constraints on action reflects a process of entropy compensation.

4.2. Introduction

Adapting human goal-directed action to different task and environmental contexts has long been viewed as the result of a confluence of *organismic*, *task*, and *environmental* constraints (Newell, 1986). Such constraints have been viewed as a means of placing restrictions on the dynamics of the perception-action system and reduce its *entropy* (Kugler, Kelso, & Turvey, 1980; Kugler & Turvey, 1987). Shaw and Turvey (1999) have raised the possibility that human action is governed by an underlying conservative process. From this perspective, human action possesses conserved quantities that are distributed across the dimensions of the action through compensation. The goal of Chapter 4 is to examine the hypothesis that entropy present at the level of the task, organism, and environmental constraints is conserved in human action.

Entropy has long been used in the characterization of human action. At the level of the organism, the probabilistic nature of human movement led Bernstein (1967) to propose that human movement could be characterized by entropy. Fitts (1954) used information entropy (Shannon, 1948) as an index of the level of difficulty of an aiming task. Hick (1952) took an information theoretic view of the environment, representing the number of stimulus-response alternatives as a log-probability, and demonstrated that reaction time increased linearly as a function of what could be viewed as environmental entropy. Moreover, tradeoffs in entropy between task and organism, as well as environment and organism, have already been found.

Harris and Wolpert (1998) showed through simulation that motor adaptation to different tasks reflects the minimization of motor noise through the modulation of the magnitude of the motor command. With the assumption that motor noise is signal

dependent, the increases in movement time when movement amplitude is increased and target width decreased are due to a reduction of motor noise. Similarly, the reduction in movement velocity in concert with a decreasing radius of curvature is reflective of a minimization of motor noise through the modulation of the magnitude of the motor command. The result is a decrease in motor entropy at the level of the organism via a constraint placed on the motor command. Given the assumption that motor variance has a constant Gaussian distribution, the model can be viewed as reflecting an entropy tradeoff or compensation between the organism and the task. Increases in task entropy through changes in amplitude, target width, or radius of curvature are compensated by a decrease in entropy at the level of the organism.

Similarly, increased environmental entropy leads to a reduction in entropy at the level of the organism. For example, Slifkin, Vaillancourt, and Newell (2000) have demonstrated that decreasing the feedback frequency in an isometric force production task leads to a decrease in Approximate Entropy (ApEn – Pincus, 1991), a measure of the sequential entropy within a time-series. This finding represents a tradeoff between the entropy in the environment and the organism. As feedback is provided with increasing frequency, more information from the environment is provided to the organism, and entropy in the environment is reduced, resulting in an increase in entropy of the force dynamics. These compensatory changes in entropy between task and organism, and environment and organism are consistent with the hypothesis that entropy is conserved across the various categories of constraint.

The main objective of this experiment is to investigate whether the compensation of motor entropy occurs systematically with changes in task and environmental entropy.

In isometric force production to a target value, visual feedback is essential in order to maintain the force output to the level of the target force even in rhythmic tasks (Sosnoff & Newell, 2005a), allowing feedback frequency to be characterized as an external source of environmental information. Continuous isometric force production also allows the study of the time-dependent entropy in muscle force output under different task and environmental constraints (Newell & Slifkin, 1998). Task entropy can thus be manipulated through the ratio of target force and force error tolerance (Kantowitz & Elvers, 1988), following from a Fitts (1954) paradigm, while the entropy of the environment can be manipulated by changing the frequency of the visual feedback provided.

It is hypothesized that the effects of task and environmental entropy on the entropy of force dynamics are compensatory, where increases in entropy at the level of the task and environment lead to decreases in entropy at the level of the organism (force dynamics). With information entropy as one of the foundations in the study of dynamic systems (Shaw, 1984) and their spatiotemporal patterns (see Haken, 2000), it can serve as a uniform metric that allows the estimation of entropy in motor dynamics, as well as that of the task (Fitts, 1954) and environment (Hick, 1952). This study will also investigate the hypothesis of entropy conservation by examining the entropy of the force output as a function of the entropies of the task and environment. This function will provide a generalized description of the relation between the entropies of the task, environment, and that of the organism.

4.3. Method

4.3.1. Participants

12 college-aged individuals (6 male, 6 female, mean age = 26 years) volunteered as participants in this study. All participants were right-hand dominant (as determined by the preferred writing hand) and were free of any neuromuscular disorders or injuries to the limbs. Informed consent was provided prior to participation, with approval for the experimental protocol from the Pennsylvania State University Institutional Review Board.

4.3.2. Apparatus

A 3-dimensional load cell (ATI Industrial Automation, Garner, North Carolina) were used to measure the force output produced by the participants (Figure 4.1). Force data were sampled at a rate of 100 Hz.

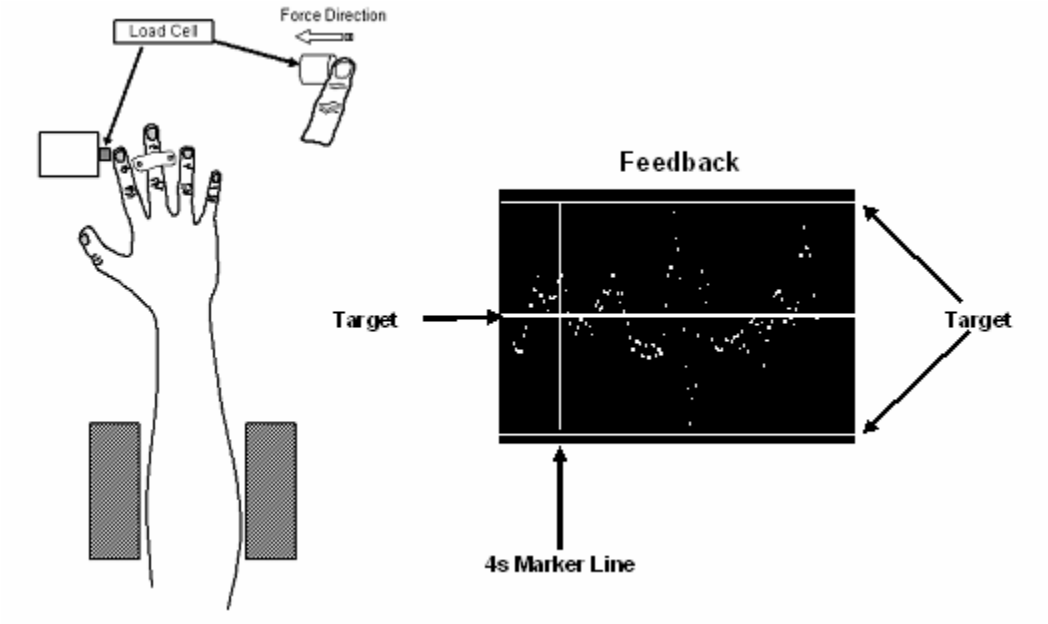

Figure 4.1. Schematic illustration of the experimental setup and load-cell orientation.

4.3.3. Procedures

MVC (maximal voluntary contraction) for each participant was determined at the beginning of the experimental session. Participants were instructed to exert maximal isometric force by pushing their index finger against the surface of the load cell toward the midline of the body as hard as possible. Each participant completed 2 MVC trials of 10s with 20s rest between each trial. The average of the highest force value produced in each trial determined the respective MVC for each individual participant.

Following the determination of MVC, each participant was asked to match their force output to 25% of their MVC. The target force level was represented as a red line against a black background on a computer screen. The computer monitor on which the visual feedback was provided possessed a screen resolution of 800 (width) × 600 (height) pixels. Online feedback of the force output (Figure 4.1) was provided via a force trajectory (plotted with white pixels) that passed from the left to right of the screen as the trial progressed. The target tolerance range was placed around the red target line, marked by two blue bands. A vertical blue line marked the completion of the first 4 s of the task, which provided the participants the opportunity to shift their force output within the target bands. Upon completion of each trial, the participant was provided with the RMSE (root mean square error) as post-trial feedback. Participants were informed that their performance in the first 4 s of the trial would not be factored into their RMSE scores. RMSE was calculated as:

$$RMSE = \sqrt{\frac{\sum (F - f_i)^2}{(n-1)}} \qquad (4.1)$$

where F is the target normal force value and f_i is the i^{th} force sample in the time series. The RMSE provided to the participants did not include performance during the first 4 s and last 1 s of the trial.

The boundary conditions of the task were defined in a manner similar to Fitts (1954), by representing the tolerance range around the target force as a signal-to-noise ratio. These ratios placed the target force within error bands of 2:1, 4:1, 8:1, 12:1, and 16:1. Each of these task levels were paired with 5 different visual feedback frequency conditions at 2.0, 3.0, 4.5, 9.0, and 16.0 Hz (Slifkin et al., 2000), yielding a total of 25 conditions. The conditions were presented to the participants in random order and participants completed 3 consecutive trials in each condition.

4.3.4. Data Analysis

The effects of the transitory forces at the beginning of the trial and the anticipation of trial termination were removed by omitting the initial 4 s and the final second. Data were smoothed with a ninth-order Butterworth low-pass filter with a cutoff frequency of 30 Hz. From the cropped and filtered *Fz* force time series from each of the trials, standard deviation (SD) and Approximate Entropy (ApEn) values were calculated. Root mean square error values were calculated for the normal force, *Fz* as a measure of the participants' performance, namely the ability to closely track the target force. Task × Environment (5 × 5) repeated measures ANOVAs were run independently on the 3 dependent variables (SD, RMSE, and ApEn) using STATISTICA (Statsoft, Tulsa, OK). Where necessary, the Greenhouse-Geisser adjustment was applied to correct for any violations of the sphericity assumption.

In order to convert the task and feedback frequency into an information theoretic framework, *information entropy* estimates were obtained from the visual feedback frequencies and signal-to-noise ratio of the force and its target bands. Information entropy (Shannon, 1948), *H*, was calculated as:

$$H = \log_2 \frac{1}{p} \tag{4.2}$$

where *p* is the probability of occurrence, with the working assumption that all events or symbols have an equal likelihood of occurring. Feedback frequency is viewed as *environmental entropy* due to the gaps between each presentation of the force output point on the display. During these time gaps in visual feedback, force output is unknown and is, therefore, uncertain allowing for environmental entropy to be estimated based on the motion-detection capacity of the human visual system. Based on the conditions of this experiment, participants were placed at a 3º visual angle, approximately.

Based on Landis (1954), the critical Flicker Fusion Threshold (FFT), which is the frequency at where a flashing dot presented to a participant becomes indistinguishable from a continuous, steady presentation, is approximately 36 Hz. Therefore, environmental entropy is estimated as $\log_2(36/\textit{Frequency})$. The visual feedback frequencies of 16.0, 9.0, 4.5, 3.0, and 2.0 Hz provide environmental entropy values of 1.2, 2.0, 3.0, 3.6, and 4.2 bits.

Similar to Fitts' Law (Fitts, 1954; Fitts & Peterson, 1964), the entropy of a motor task can be measured as a signal-to-noise ratio that can be obtained from movement amplitude and target width. The target force level in this experiment is analogous to the movement amplitude, and the bands placed around the target force are similar to the target width in Fitts' Law. For example, if the desired force was 10 N, a tolerance range

that allows errors of 1.25 N above and below the target line (2.5 N in total) has a signal-noise ratio of 4:1. A 12:1 ratio would mean a margin of error 0.2 N above and 0.2 N below the target line. Here, the signal-noise ratios employed as task constraints were 2:1, 4:1, 8:1, 12:1, and 16:1. By obtaining the base-2 logarithm of these ratios, these values yield task entropies of 1.0, 2.0, 3.0, 3.6, and 4.0 bits.

Approximate Entropy (ApEn – Equation 4.3) is a measure of the irregularity of a time-series (cf. Pincus, 1991). ApEn is also a measure of time-dependent or sequential entropy (Beltrami, 1999) and here, the base-2 logarithm is employed in order to obtain ApEn values in bits. As recommended by Pincus (1991), the value of m was set at 2, while r was set to 0.2 of the standard deviation of the time-series.

$$ApEn(\vec{X}, m, r) = \log_2\left[\frac{C_m(r)}{C_{m+1}(r)}\right] \qquad (4.3)$$

In this algorithm, $C_m(r)$ and $C_{m+1}(r)$ provide the average count of the recurrence of vectors of length m and m+1 within a given time-series, X. In regular/predictable time series, values of $C_m(r)$ will be similar to $C_{m+1}(r)$, as vectors of shorter length repeat with equal likelihood to longer ones. Higher ApEn values reflect a more irregular time series, where the predictability of subsequent events in the time-series is low, as the differences between vectors of length m and m+1 within the time-series are greater.

ApEn is an entropy measure that is obtained from the logarithm of the probability ratio of $C_{m+1}(r)$ to $C_m(r)$, which is inverted to log $(1/p)$ in order to obtain positive values. As the conservation law postulation is dependent on the idealized situation of the continued achievement of the task goal, the probability here must be contingent upon the maintenance of the target force within the boundaries of the task constraint and hence be made conditional. Conditional probabilities provide the likelihood that an event, x occurs

given the condition that another, *y* has occurred, making the conditional probability, $p(x|y)$ equal to $p(x)$ divided by $p(y)$.

In the context of the current experiment, ApEn will be calculated as:

$$ApEn(\vec{X}, m, r) = \log_2 \left[\frac{C_m(r)}{C_{m+1}(r)} \times \frac{N_g}{N_{Fz}} \right] \quad (4.4)$$

ApEn is made conditional by multiplying the probability of the force output being maintained within the boundaries of the task. This probability can be obtained from the ratio of the total number of data points within the force time-series, N_{Fz} to the number of data points that were within the target bands defined by the task constraint, N_g. As Pincus (1991) designed ApEn to return positive values, it is a log $(1/p)$ calculation, rather than dividing by the probability of achieving the task the ratio is inverted and then multiplied by $\frac{C_m(r)}{C_{m+1}(r)}$.

From these conditional ApEn data, nonlinear regression will be applied to obtain coefficients to generate a 3-dimensional surface that describes the effects of the task and environment on the ApEn of the force output from a function similar to the one presented in Newell, Liu, and Mayer-Kress (2005). This function also holds common elements to the quadratic surface presented in de Ruyter van Steveninck, Bialek, Potters, Carlson, and Lewen (1996):

$$H_{org} = k - aH_{task}^2 - bH_{env}^2 \quad (4.5)$$

Here, *k* is the intercept, and *a* and *b* are the coefficients obtained from the fit, and H_{task} being the entropy of the task, and H_{env} the entropy of the environment. These coefficients will be obtained from lines of best fit for the averaged effects of the entropies of the task and environment on ApEn, the entropy of the organismic output, represented as the

elevation of the surface, H_{org}. The intercepts obtained from the individual functions fits applied to the task and environmental entropies are averaged to obtain k.

4.4. Results

The mean MVC generated by the participants was 26.3 ± 9.4 N.

Repeated measures ANOVA found significant effects of Environment ($F(4,44) = 20.9$, $p<0.0001$) and Task ($F(4,44) = 2.8$, $p = 0.0394$) on the SD of the force output. The Task × Environment interaction was not significant ($p = 0.7891$). Figure 4.2 provides an illustration of the means at different levels of Task and Environmental conditions along with the results of the Tukey post-hoc tests.

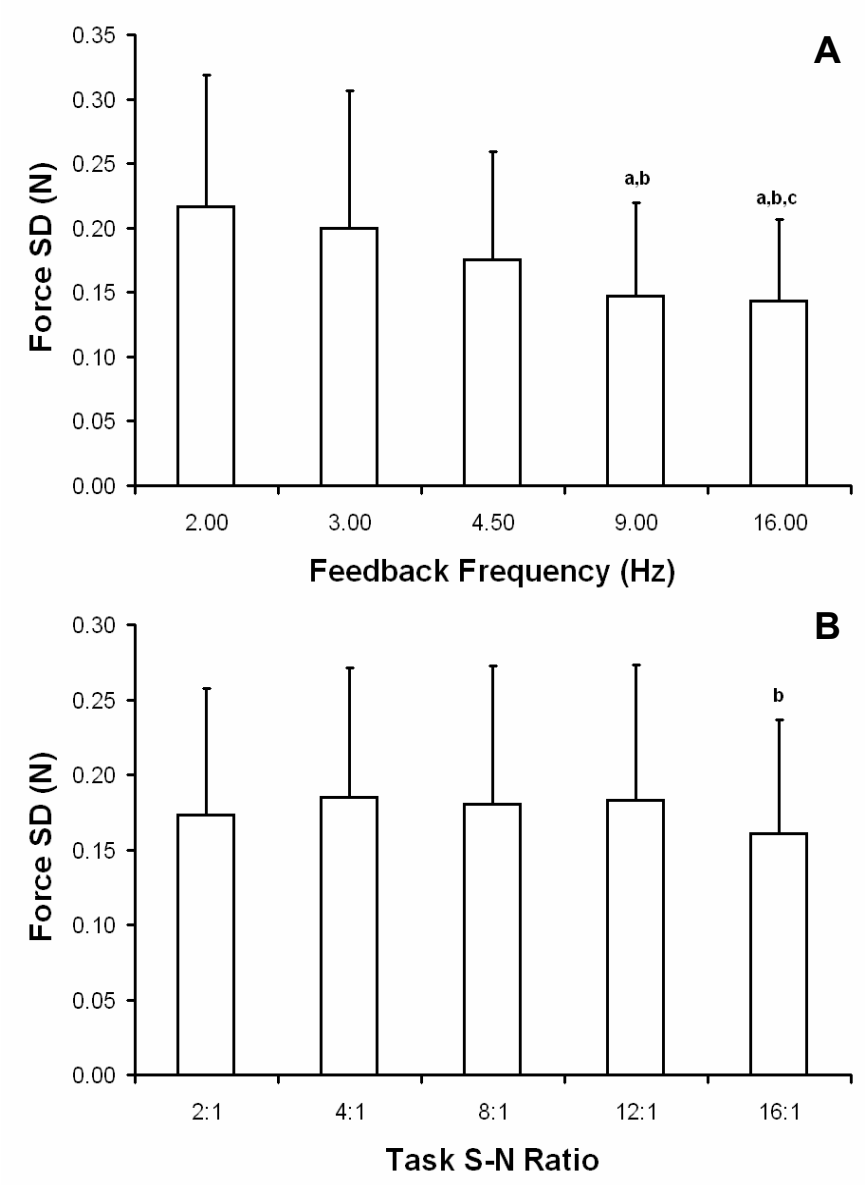

Figure 4.2. Magnitude of variability under the effect of feedback frequency (A) and task constraint (B). Significant Tukey comparisons ($p<0.05$) are marked by the letters above each bar. Note: a, b, and c superscripts denote significantly different from 2, 3, and 4.5 Hz feedback frequencies (A). b superscript denotes significantly different from a task signal-to-noise ratio of 4:1. Error bars mark 1 SD (between-subjects).

Similar results were obtained for RMSE and both the effects of the Environment ($F(4,44) = 18.2$, $p<0.0001$) and Task ($F(4,44) = 3.1$, $p = 0.0258$) were significant, while the interaction was not significant ($p = 0.8236$). The results of the Tukey post-hoc tests on the main effects on RMSE are presented in Figure 4.3.

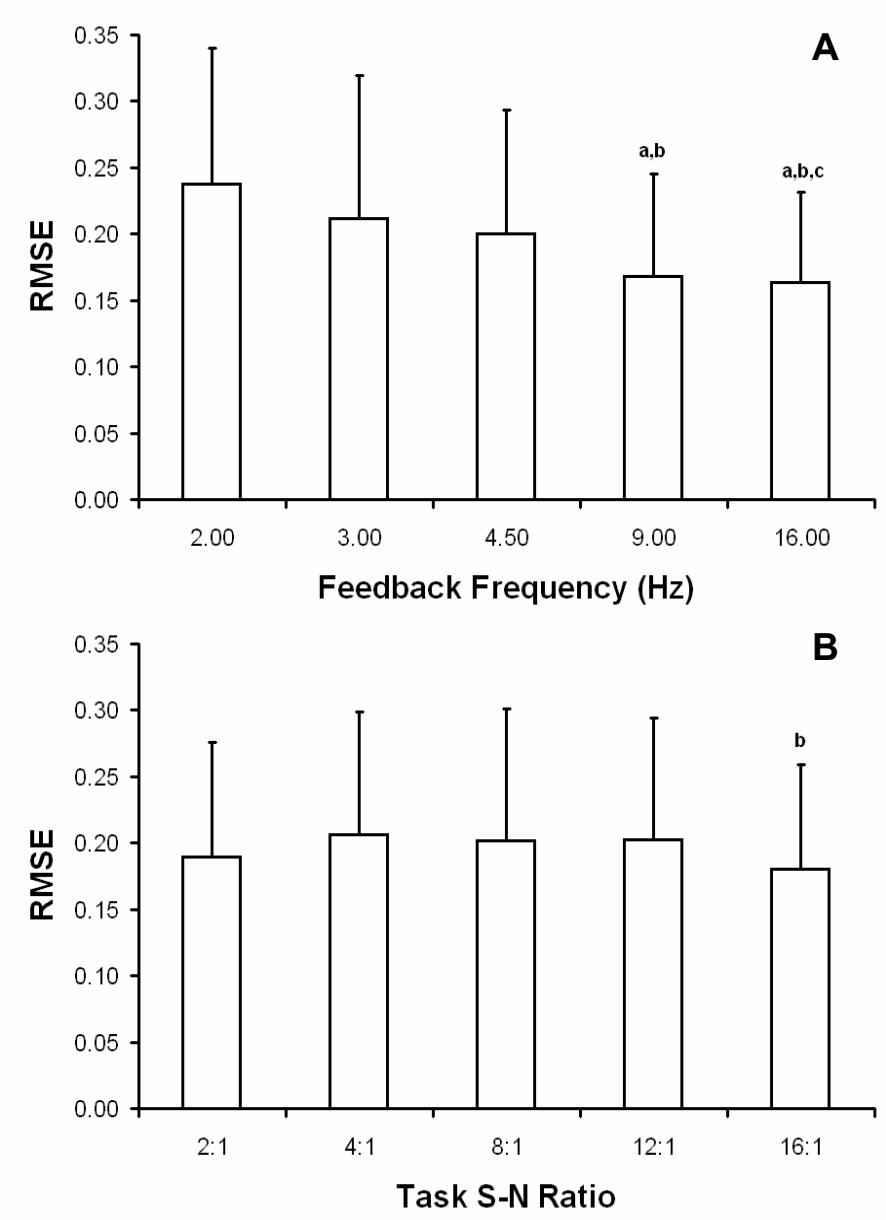

Figure 4.3. RMSE under the effect of feedback frequency (A) and task constraint (B). Significant Tukey comparisons ($p<0.05$) are marked by the letters above each bar. Note: a, b, and c superscripts denote significantly different from 2, 3, and 4.5 Hz feedback frequencies (A). b superscript denotes significantly different from a task signal-to-noise ratio of 4:1. Error bars mark 1 SD (between-subjects).

Significant effects of Task ($F(4,44) = 55.9$, $p<0.0001$) and Environment ($F(4,44) = 14.2$, $p<0.0001$) on ApEn were also found with a non-significant ($p = 0.5764$) interaction. The effects of the different environmental conditions under different task conditions and vice versa on ApEn are presented in Figure 4.4. ApEn increased with feedback frequency and decreased with increasing task constraint.

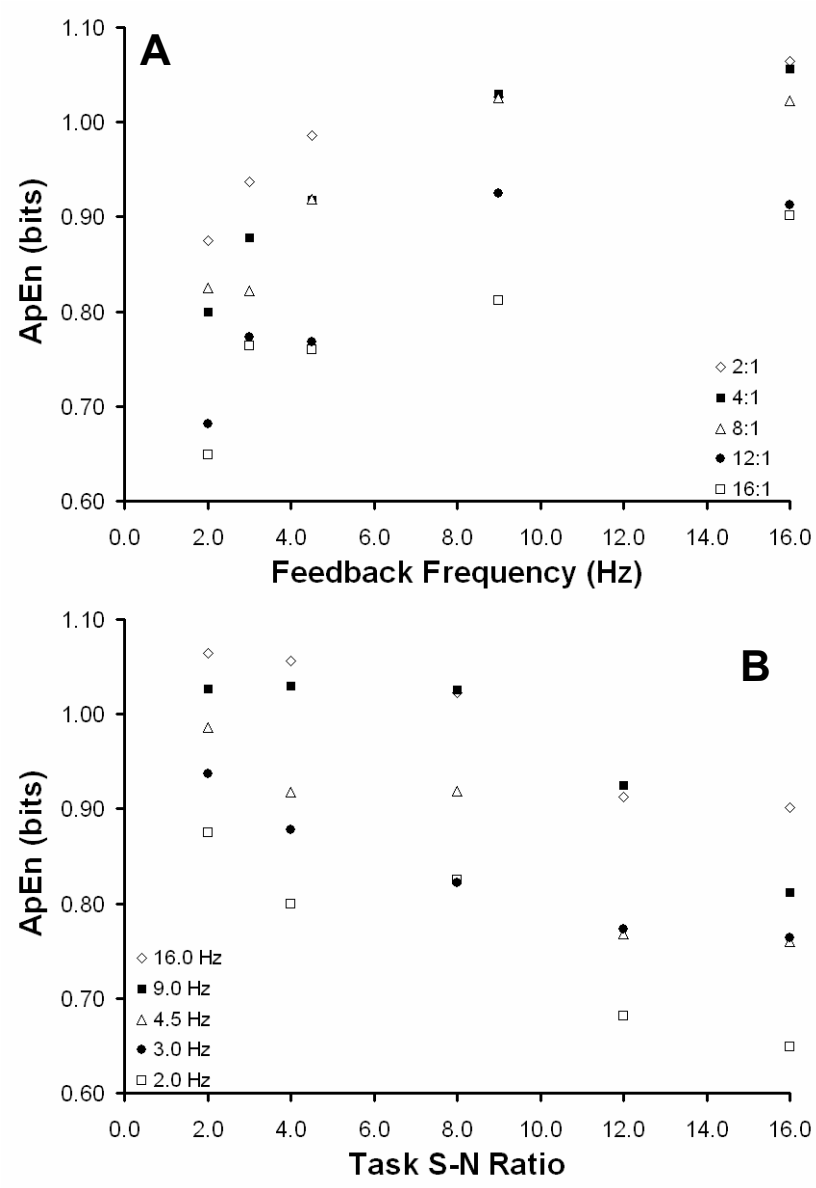

Figure 4.4. Figure 4.4.A presents the effects of feedback frequency on ApEn under different task constraints. Figure 4.4.B presents the effect of task constraint when participants are provided with different feedback frequencies.

ApEn, represented as functions of the entropies of the environment and task are presented in Figures 4.5.A and 4.5.B. The upper panel presents the average effect of the environment on ApEn while the lower panel illustrates the average effect of the task. The r^2-values for the functions fitted to the environment and task were 0.93 and 0.98, respectively. From each of these fits, the average intercept and each of the coefficients were applied to obtain the surface presented in Figure 4.5.C. This surface is correlated to the data with an r^2-value of 0.92.

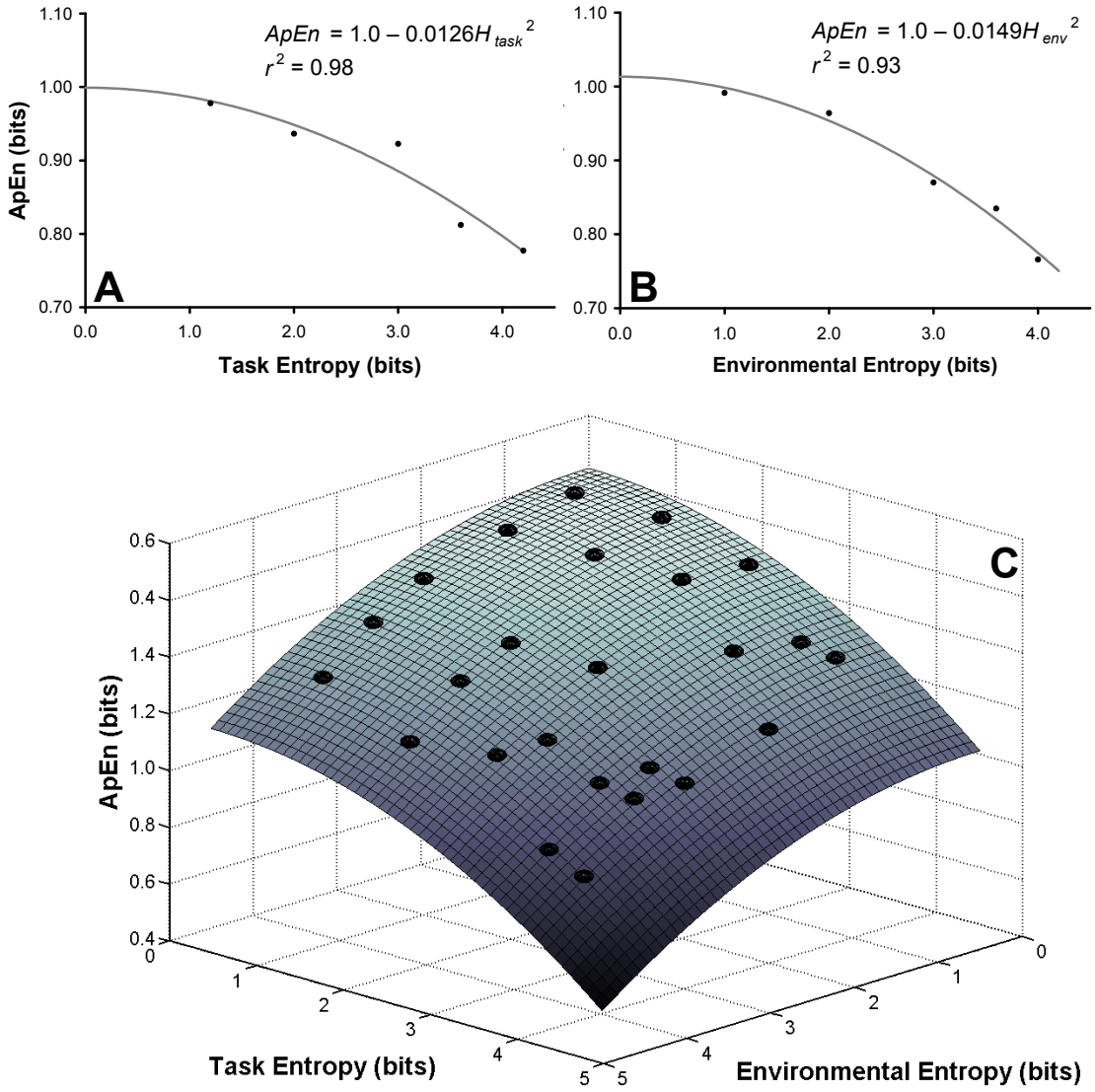

Figure 4.5. Feedback frequency and task constraint represented as environmental (A) and task (B) entropies. The best fitting functions and r^2 values are also provided (Note: H_{env} = environmental entropy; H_{task} = task entropy). Quadratic surface generated from the coefficients presented in Figure 4.5.C. This surface is correlated to the data with an r^2 value of 0.92.

4.5. Discussion

The results of this study provide support for the postulation of compensatory effects of the entropy of the task and environment on the entropy of force dynamics.

Environmental and task entropy significantly affected both the magnitude and dynamic structure of the force output. These findings support the general view that human action is a product of the confluence of task, organismic, and environmental constraints (Newell, 1986). More specifically, the findings also support the hypothesis that conserved quantities are present in human action (Shaw & Turvey, 1999) and provide preliminary evidence for entropy as a candidate for a conserved quantity across the three categories of constraint in human action.

4.5.1. Distributional Properties of Force Output

Consistent with prior studies on the effects of visual feedback on the magnitude of variability in force output (Slifkin et al., 2000; Sosnoff & Newell, 2005b) the variability of force output decreased nonlinearly with increasing feedback frequency. The effect of the availability of visual feedback on RMSE was essentially identical to its effect on SD. This shows that not only is variability reduced with increasing feedback frequency but accuracy, as in the ability to remain close to the target line is also enhanced.

The effect of increased task constraint through reductions in the error tolerance range, however, was less clear than that of the feedback frequency. Here, only one of the post-hoc comparisons proved to be significant ($p<0.05$), with this difference being between the signal-to-noise ratios of 4:1 and 16:1. This shows that at the high task constraint (narrow tolerance range around the target force), performance was improved, reflecting decreased variability and increased ability to track the target force.

4.5.2. Entropy in Force Dynamics

The effect of feedback frequency on ApEn of force dynamics is similar to previous findings (Slifkin, Vaillancourt, & Newell, 2000; Sosnoff, Jordan, & Newell, 2005; Sosnoff & Newell, 2005). There was a nonlinear increase in the entropy of the force dynamics with higher feedback frequency. Increasing the task constraint produced a similar, but opposite effect on ApEn to that of feedback frequency, with a nonlinear decrease in ApEn to the narrowing of the target bands. The lack of a significant Task × Environment interaction demonstrates that the conditional probability correction for ApEn introduced here did not significantly alter the effects of visual feedback frequency on ApEn as found in Slifkin et al. (2000), but remains able to account for changes in the participants' ability to remain within the task constraints. These findings show that as task and environmental entropy are increased, the entropy of the force dynamics decreases.

When viewed in terms of the construct of entropy, the ApEn as functions of task and environmental entropy taken independently converge to a similar intercept and possess generally similar coefficients (Figure 4.5). The central relation is that as the entropy of the task and environment are increased, the entropy of the motor output is decreased. This surface of entropy relations highlights the concept of entropy conservation through compensation. Indeed, the surface in Figure 4.5.C demonstrates that when both task and environmental entropy are at their lowest, the organismic (force output) entropy achieves its peak, represented by the intercept, *k*. At the highest levels of task and environmental entropy, the entropy of force dynamics is at its lowest, as the surface converges toward its base. The compensation of entropy is reflected on the

surface, where low levels of task entropy coupled with a high level of environmental entropy result in a similar level of entropy of the force dynamics as a low level of environmental entropy coupled with a high level of task entropy.

It should be noted that the sum of quadratic functions provides a mathematical identification of the symmetry or equality between the organism, and the task and environment. The classic equation of the conservation of momentum describes the relation between masses, m, and the velocities, v:

$$m_1 v_1 = (m_1+m_2)\, v_2 \qquad (4.6)$$

can be reorganized to $(m_1+m_2)\, v_2 - m_1 v_1 = 0$, where the product of the momenta equal a constant, zero. Similarly, in the context of the conservation of entropy in human action, the sum of quadratic functions (Equation 4.5 with the coefficients a and b removed for the purpose of simplicity) can be represented as:

$$k = H_{org} + H_{task}^{\,2} + H_{env}^{\,2} \qquad (4.7)$$

where the sum of the entropies equal a constant value, k. Thus, Equation 4.7 serves as a generalized mathematical description of the conservation of entropy. This also affords the postulation of entropy as a possible candidate for a conserved quantity in human action.

Similarities in the coefficients and intercepts obtained from the fitted functions point to a general symmetry between the effects of task and environmental entropy on the entropy of the motor output dynamics. This finding of near symmetry provides support for the estimation of environmental entropy using the Flicker-Fusion Threshold (Landis, 1954) and the view of representing task difficulty as a signal-to-noise ratio (Fitts, 1954). The key issue here, however, is that the effect of increasing task difficulty need not

necessarily result in a speed-accuracy tradeoff, but rather one of a reduction in motor entropy with increasing task entropy, in keeping with the model presented in Harris and Wolpert (1998). Furthermore, these recent findings lead to a view that the compensatory changes in motor entropy are not due to the minimization of motor variance with respect to the task demands through motor command modulation, but rather, reflect changing levels of entropy across the organism, task, and environment guided by a natural conservation law.

Chapter 5

Entropy Compensation across the Constraints on Coordination

5.1. Abstract

The effects of task and environmental entropy on bimanual isometric force output were investigated. Participants produced two-finger force output to a constant level under different task (force target width) and environmental (feedback frequency) conditions. Significant effects of the task and environment, as well as a task × environment interaction on the relative phase entropy were found. Information entropy of the relative phase of the force output of the two fingers, made conditional upon the probabilities of achieving the goal, decreased nonlinearly with increasing entropy of the task and environment. The compensatory nature of the effects of task and environmental entropy on the entropy of force dynamics is represented by a quadratic surface.

5.2. Introduction

Movement coordination patterns that are generated to achieve a given action goal arise from the confluence of task, organismic, and environmental constraints (Newell, 1986). Indeed, one of the most remarkable aspects of the human motor system is its ability to adapt its output, and more importantly, the structure of its variability to a variety of task and environmental contexts (Newell & Slifkin, 1998). The inherently probabilistic nature of human movement and the resulting between- and within-trial variation can thus be assessed using measures of entropy (Bernstein, 1967).

Inherent in action is a level of uncertainty in whether or not the task is completed (cf. Fitts, 1954). Similarly, a level of entropy exists in the environment, leading, for example, the actor to require information from the environment in order to execute a given action (cf. Hick, 1952; Hyman, 1953). And, when constraints are placed upon the motor system, the entropy of the movement in action is often reduced (Kugler, Kelso, & Turvey, 1980; Kugler & Turvey. 1987). The goal of this study is to examine whether entropy of the force output in a bimanual isometric force task will change systematically and in a compensatory manner with respect to the entropies of the task and environment.

In bimanual movements, the stability of the coordination pattern between 2 limbs can be characterized by the standard deviation (Schöner, Haken, & Kelso, 1986) or by the shape of the distribution (Turvey & Carello, 1996) of the relative phase between the moving limbs. The changes in coupling between 2 limbs or limb segments reflect the addition or removal of organismic constraints, with a resulting reduction or increase in the entropy of the movement pattern. As additional constraints are placed upon the motor

system, the independence of the components or degrees of freedom of the motor system is decreased (Kugler et al., 1980).

With respect to the entropy of the task, Harris and Wolpert (1998) modeled the speed-accuracy tradeoff (Fitts, 1954) as well as the 2/3 power law (Lacquaniti, Terzuolo, & Viviani, 1983) using a minimum motor variance principle. Harris and Wolpert (1998) demonstrated with the minimum variance model that the increase in movement time (Fitts' Law) and reduction in movement velocity (2/3 power law) could be explained by the modulation of the magnitude of the motor command responsible for movement initiation (Schmidt, Zelaznik, Hawkins, Frank, & Quinn, 1979). Thus, motor variance can be adjusted to match the task demands by increasing or reducing the magnitude of the motor command. The simulation results obtained by Harris and Wolpert (1998) could be viewed as an example of increases in task difficulty or entropy leading to a tradeoff and a decrease in entropy of the motor output, if the assumption of a Gaussian distribution of the variance is upheld.

Complementary tradeoffs have also been noted between environmental and motor entropy. For example, altering properties of visual feedback has been shown to affect the dynamics of isometric force output. Reducing the visual information presented on a computer monitor leads to a decrease in entropy in the motor output in isometric force production tasks, as indexed by a decrease in Approximate Entropy (Sosnoff & Newell, 2005a, 2005b). During two- and three-finger prehension tasks, Sosnoff, Jordan, and Newell (2005) found a similar effect of decreased visual feedback on the coupling between the fingers during grasping. As the rate of visual feedback was decreased,

synchrony between the forces produced by the fingers increased (as indexed by Cross-Approximate Entropy), reflecting a decrease in the entropy of the motor output.

Bracewell, Wing, Soper, and Clark (2003) have shown that the correlation between grip forces produced during a bimanual grasping task was higher when the unpredictability of the object load was increased. Bracewell et al. (2003) proposed that these results were reflective of greater constraint at the coordinative level. These findings provide evidence for tradeoffs between environmental entropy and the entropy of the movement patterns produced by the organism. Thus, for a given action that is performed under different task and environmental constraints, it is expected that the changes in the motor output, as measured by the information entropy of the coordination dynamics, will be systematic with the entropy of the task and environment.

The adaptation of coordination patterns to different task and environmental contexts may reflect the conservation of entropy, with compensatory effects at both the level of the task and environment. Shaw and Turvey (1999) proposed that conserved quantities are present in human movement. Empirically, a conserved quantity is found to be distributed across the various dimensions of the action through compensatory processes. Such compensations in entropy have been previously demonstrated as tradeoffs in entropy between the organism, environment, and task. With a working assumption that entropy is present at each category of constraint and that compensation reflects conservation (Shaw & Turvey, 1999), entropy is a possible candidate for being a conserved quantity in human action.

In summary, Chapter 5 investigates the hypothesis that as entropy of the task or environment is increased, entropy of the coordinated isometric force output would be

reduced. Furthermore, the effects of the changes in task and environmental entropy on the motor pattern are hypothesized to be compensatory. As such, a high level of task entropy coupled with a low level of environmental entropy will have a similar effect on the entropy of motor output as that of an action performed with low task entropy and high environmental entropy. Information entropy can be applied as the uniform metric for characterizing the task, environment, and organism. Information entropy is based on probabilities and has long been employed in the study of dynamic systems (Shaw, 1984) and as a means of characterizing spatiotemporal patterns (Haken, 2000). Consistent with other conservation concepts, the hypotheses presented here are based on an idealization, in this case in action where the movement goal in action is always achieved. Situations where the goal is not achieved are accounted for through the use of conditional information entropy.

5.3. Method

5.3.1. Participants

12 individuals between the ages of 19 and 33 years (6 male, 6 female, mean age = 26 years) volunteered as participants in this study. All participants were right-hand dominant (as determined by the preferred writing hand) and were free of any neuromuscular disorders or injuries to the limbs. Informed consent was provided prior to participation, with approval for the experimental protocol from the Pennsylvania State University Institutional Review Board.

5.3.2. Apparatus

Two 3-dimensional load cells (ATI Industrial Automation, Garner, North Carolina) measured the forces produced by the participants. Force data were collected with a sample rate of 100 Hz and smoothed with a ninth order Butterworth low-pass filter with a cutoff frequency of 30 Hz. The experimental setup is presented in Figure 5.1.

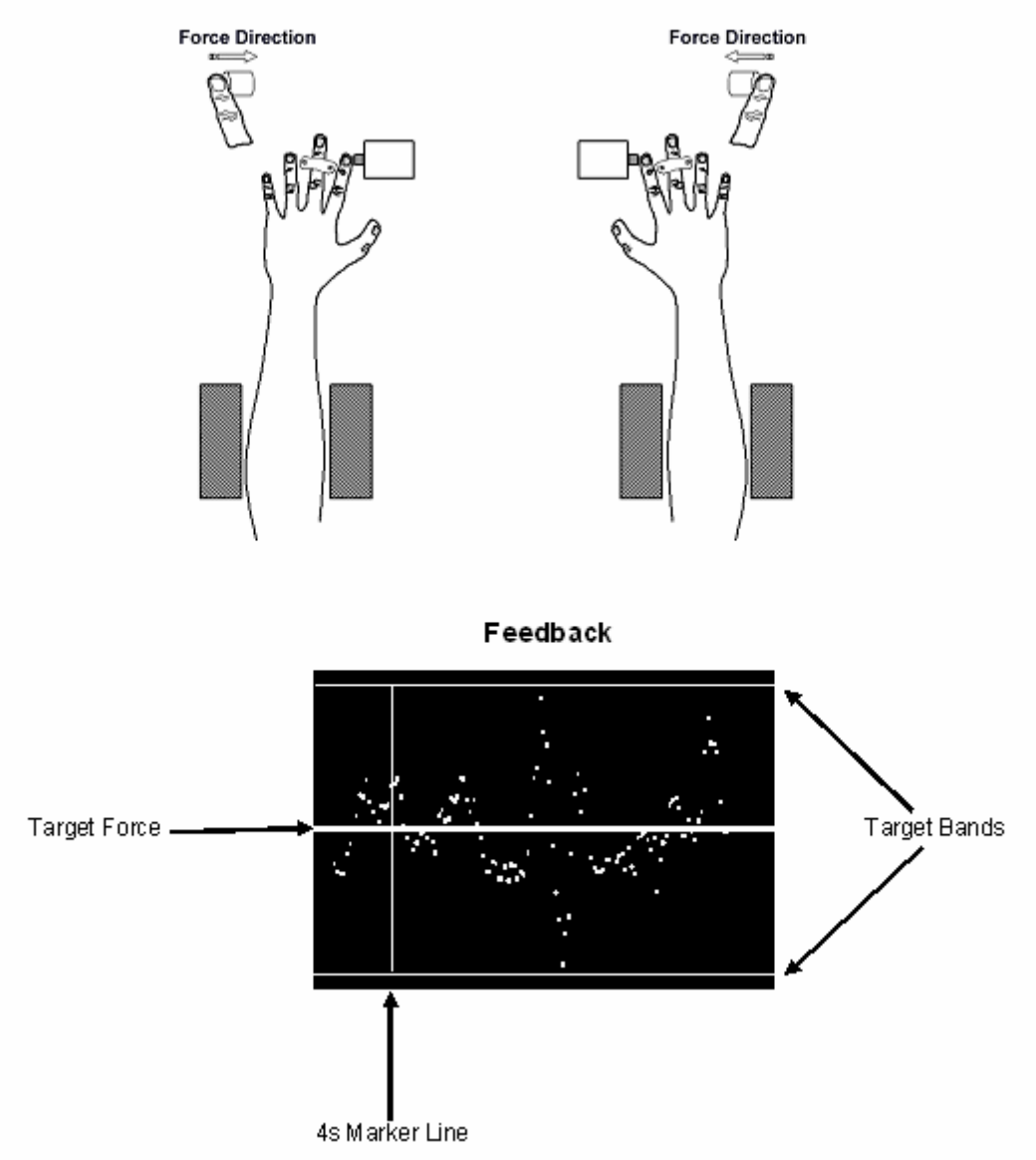

Figure 5.1. Illustration of the experimental setup and generation of bimanual isometric force through finger abduction.

5.3.3. Procedures

Maximal voluntary contraction (MVC) was determined for each participant at the beginning of the experimental session. Participants were instructed to exert maximal isometric force by pushing their index fingers against the surfaces of load cells simultaneously with as much force as possible. Force was generated by pushing against the load cells toward the midline of the body. Each participant completed 2 MVC trials of 10s with 20s rest between each trial. The average of the highest force value produced in each trial determined the respective MVC for each individual participant.

Following the determination of MVC, each participant was asked to match the target line with the force output from both fingers that was 25% of their MVC. The participants were reminded that they were allowed to employ any coordination strategy between their 2 index fingers, as long as they remained as close to the target line while remaining within the bounds of the target bands as much as possible.

The computer monitor on which the visual feedback of the total force was provided possessed a screen resolution of 800 (width) × 600 (height) pixels. In order to control for the effects of strength and MVC on the sensitivity of visual feedback, the pixel-to-Newton (*p/N*) ratios were normalized for all participants, setting the screen height to be equivalent to the target force. Thus, the *p/N* ratios were fixed at 600 pixels per Newton of target force. Online feedback regarding force output (Figure 5.1) was provided via a force trajectory (plotted with white pixels) that passed from the left to right of the screen as the trial progressed. Target bands (colored blue) were placed around the red target line. A vertical blue line marked the completion of the first 4 s of the task, which provided the participants with the opportunity to stabilize their force

output within the target bands. Upon completion of each trial, participants were provided with the RMSE (root mean square error) as post-trial feedback. RMSE was calculated as:

$$RMSE = \sqrt{\frac{\sum (F - f_i)^2}{(n-1)}} \tag{5.1}$$

where F is the target normal force value and f_i is the i^{th} force sample in the time series.

The boundary conditions of the task were defined in a manner similar to Fitts (1954), by representing the bands around the target force as a signal-to-noise ratio. These ratios placed the target force within error bands of 2:1, 4:1, 8:1, 12:1, and 16:1. Each of these task levels were paired with 5 different visual feedback frequency conditions at 2.0, 3.0, 4.5, 9.0, and 16.0 Hz (Slifkin et al., 2000), yielding a total of 25 conditions. The conditions were presented to the participants in random order and participants completed 3 blocked trials in each condition.

5.3.4. Data Analysis

Effects of the transitory forces at the beginning of the trial and the anticipation of trial termination were removed by omitting the initial 4 s and final second. For every trial, mean and SD were obtained from the cropped and filtered force time-series of the total force. Root mean square error values were calculated for the total force, *Fz* as a measure of the participants' performance, namely the ability to closely track the target force. Task × Environment (5 × 5) repeated measures ANOVAs were run on the 2 dependent variables (RMSE, and relative phase entropy) using STATISTICA (Statsoft, Tulsa, OK). Greenhouse-Geisser adjustments were employed in order to correct for violations of the assumption of sphericity.

In order to convert the task and feedback frequency into an information theoretic framework, *information entropy* or *entropy* estimates were obtained from the visual feedback frequencies and signal-to-noise ratio of the force and its target bands. Information entropy (Shannon, 1948), *H*, is calculated as:

$$H = \log_2 \frac{1}{p} \qquad (5.2)$$

where *p* is the probability of occurrence, assuming an all events or symbols have an equal likelihood of occurring. Feedback frequency is viewed as *environmental entropy*, which results in gaps between each presentation of the force output point on the display. Visual feedback in this case can be viewed as an external source of information, as the constant force production task cannot be performed using tactile and proprioceptive information alone, as force begins to degrade as quickly as 0.5s after the withdrawal of vision (Vaillancourt & Russell, 2002). During these time gaps in visual feedback, force output is unknown and is, therefore, uncertain allowing for environmental entropy to be estimated based on the motion-detection capacity of the human visual system.

The participants were seated at a distance that resulted in a 3º visual angle from the computer display, approximately. Based on Landis (1954), the critical Flicker Fusion Threshold (FFT), which is the frequency at where a flashing dot presented to a participant becomes indistinguishable from a continuous, steady presentation, is approximately 36 Hz. Therefore, environmental entropy is estimated as $\log_2(36/\mathit{Frequency})$. The visual feedback frequencies of 16.0, 9.0, 4.5, 3.0, and 2.0 Hz provide environmental entropy values of 1.2, 2.0, 3.0, 3.6, and 4.2 bits.

Similar to Fitts' Law (Fitts, 1954; Fitts & Peterson, 1964), the entropy of a motor task can be measured as a signal-to-noise ratio that can be obtained from movement

amplitude and target width. The target force level in this experiment is analogous to the movement amplitude, and the bands placed around the target force are similar to the target width in Fitts' Law (Kantowitz & Elvers, 1988). For example, if the desired force was 10 N, a bandwidth that allows errors of 1.25 N above and below the target line (2.5 N in total) has a signal-noise ratio of 4:1. A 12:1 ratio would mean a margin of error 0.2 N above and 0.2 N below the target line. Here, the signal-noise ratios employed as task constraints were 2:1, 4:1, 8:1, 12:1, and 16:1. By obtaining the base-2 logarithm of these ratios, these values yield task entropies of 1.0, 2.0, 3.0, 3.6, and 4.0 bits.

Entropy in the coordination between the 2 fingers was calculated through the information entropy of the continuous relative phase of the force outputs. Phase angles for the force traces produced by each finger were obtained from the arctangent of the normalized force and its normalized first derivative. Relative phase was determined from the difference between the phase angles of the left and right fingers. Frequency histograms provided the probability distributions of the relative phase time-series for each trial. The histograms were bounded between -360º and 360º, with equally sized bins of 30º. From the probabilities within each bin, the information entropy, H (Shannon, 1948), was calculated using the equation:

$$H = -\sum p_i \log_2 p_i \qquad (5.3)$$

where p_i represents the probability of occurrence within the i^{th} bin. As with ApEn, in order to respect the fact that the participants will not always remain within the boundaries of the task, the information entropy must be made conditional as well. In order to achieve this, the probability of remaining within the task (N_g/N_{TOT}), represented as p_g,

must be introduced into the equation. Thus, the conditional entropy of the relative phase is:

$$H_{cond} = -\sum p_g p_i \log_2 p_i \quad (5.4)$$

From these conditional entropy data, a 3-dimensional surface that describes the effects of the task and environment on the entropy of the coordination pattern will be generated from a function similar to Newell, Liu, and Mayer-Kress (2005) and de Ruyter van Steveninck, Bialek, Potters, Carlson, and Lewen (1996):

$$H_{org} = k - a_{task}H_{task}^2 - a_{env}H_{env}^2 \quad (5.5)$$

H_{task} is the entropy of the task, and H_{env} represents the environmental entropy, and H_{org} represents the entropy in the coordination pattern. With k as the intercept, a_{task} and a_{env} are the coefficients obtained through nonlinear regression. These coefficients will be obtained from lines of best fit for the averaged effects of the task and environment on H_{org} (Equation 5.5), which represents the entropy of the organismic output, H_{org}. Thus, the task effect will be fitted as $H_{org} = k - a_{task}H_{task}^2$ and the effect of the environment will be $H_{org} = k - a_{env}H_{env}^2$. The intercept will be averaged across the fits applied to the task and environment for the generation of the surface, in order to insure that the data points remain above the surface. This function also provides a mathematical description for a conservative function, as the sums of the entropies will equal a constant, k, when the equation is rearranged to $H_{org} + a_{task}H_{task}^2 + a_{env}H_{env}^2 = k$.

5.4. Results

The mean MVC generated by the participants was 60.5 ± 19.8 N. The participants were required to produce and maintain an average target force of 15.1 N (25% of MVC).

The effects of the Environment ($F(4,44) = 19.6$, $p<0.0001$) and Task ($F(4,44) = 5.2$, $p=0.0016$) on RMSE were significant, while the Task × Environment interaction marginally failed the traditional level of significance ($p=0.0562$). The results of the Tukey post-hoc tests for the main effects are presented in Figure 5.2. A Tukey post-hoc test of the main effect of the Environment on RMSE revealed that RMSE was significantly higher at 2.0 Hz feedback frequency when compared to all the other conditions. RMSE was also significantly lower at 16 Hz when compared to 2.0, 3.0, and 4.5 Hz. For the Task main effect, the Tukey post-hoc test revealed a significant difference between the extreme conditions of the task, namely ratios of 2:1 and 16:1 as well as a significant difference between the task constraint ratios of 8:1 and 16:1.

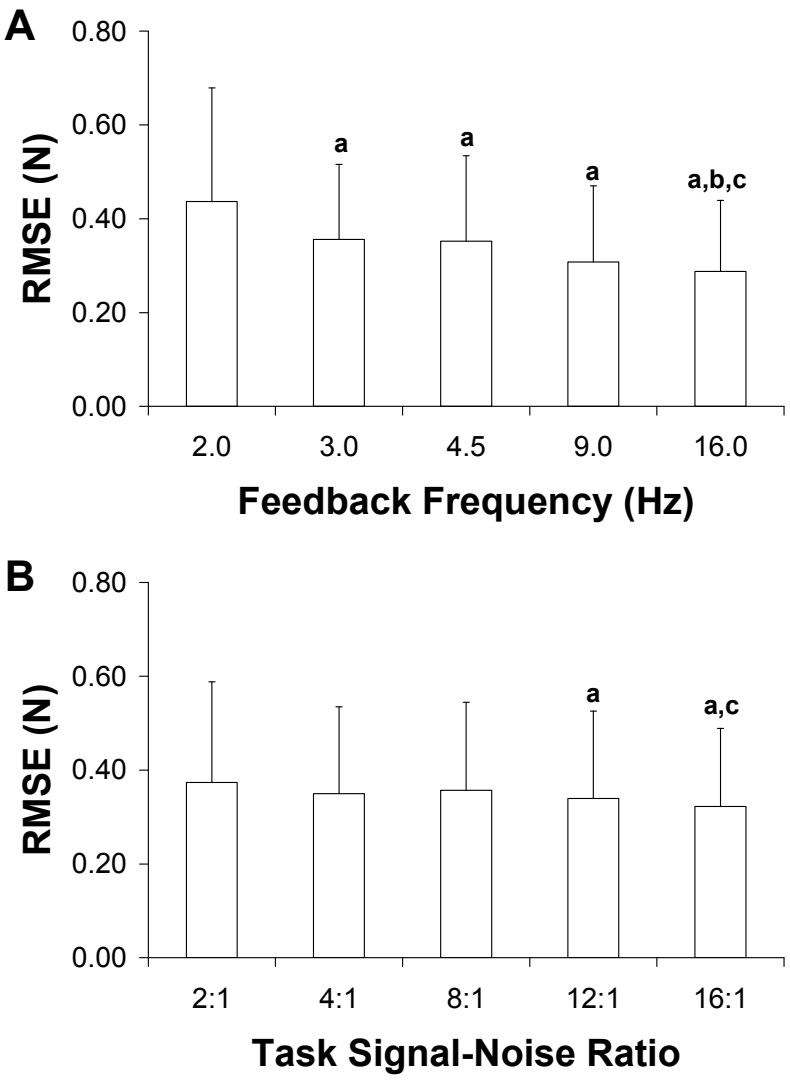

Figure 5.2. RMSE under the effect of feedback frequency (A) and task constraint (B). Significant Tukey comparisons (p<0.05) are marked by the letters above each bar. Note: a, b, and c superscripts denote significantly different from 2, 3, and 4.5 Hz feedback frequencies (A). a, and c superscripts denote significantly different from a task signal-to-noise ratios of 2:1 and 8:1 (B). Error bars mark 1 SD (between-subjects).

For relative phase entropy, the main effects of Task (F(4,44) = 55.9, p<0.0001) and Environment (F(4,44) = 14.2, p<0.0001), as well as the Task × Environment interaction were significant (F(16,176) = 2.8, p=0.0005). Exemplar frequency histograms from a single participant producing isometric force under combinations of the extreme task (2:1 and 16:1) and environmental (16 Hz and 2 Hz) conditions are presented

in Figure 5.3. This figure shows that as the error tolerance bands are narrowed and the feedback frequency reduced, the distribution of relative phase values becomes more peaked. The probability of remaining within the error tolerance bands, (N_g/N_{TOT}) is also decreased with the increased task constraint and reduced visual feedback frequency.

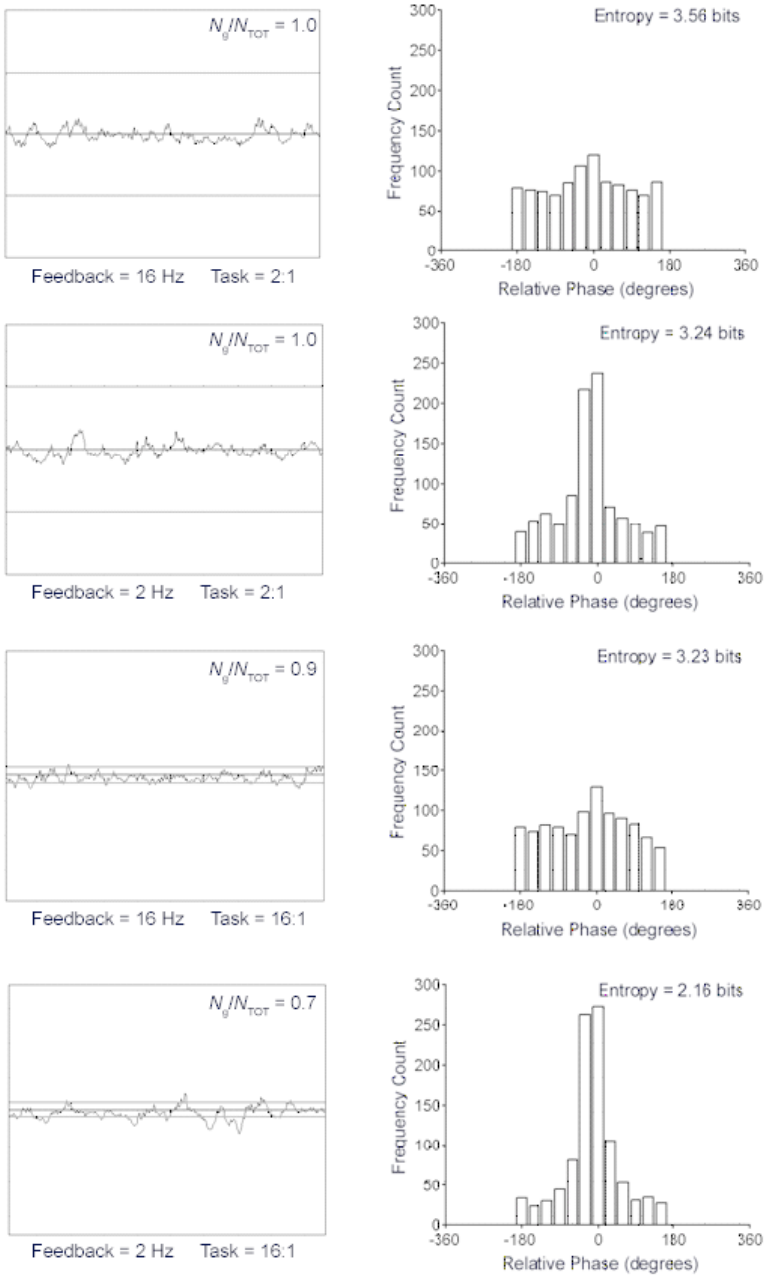

Figure 5.3. Exemplar force output (left columns) and frequency histograms (right column) from a single participant.

The effects of the environment under different task conditions and vice versa on relative phase entropy are presented in Figure 5.4. In general, relative phase entropy increased with feedback frequency and decreased with increasing task constraint. Figure 5.4 also shows that the increase in relative phase entropy with feedback frequency is mediated by the task constraint. Similarly, the decrease in relative phase entropy with increased task constraint is mediated by feedback frequency.

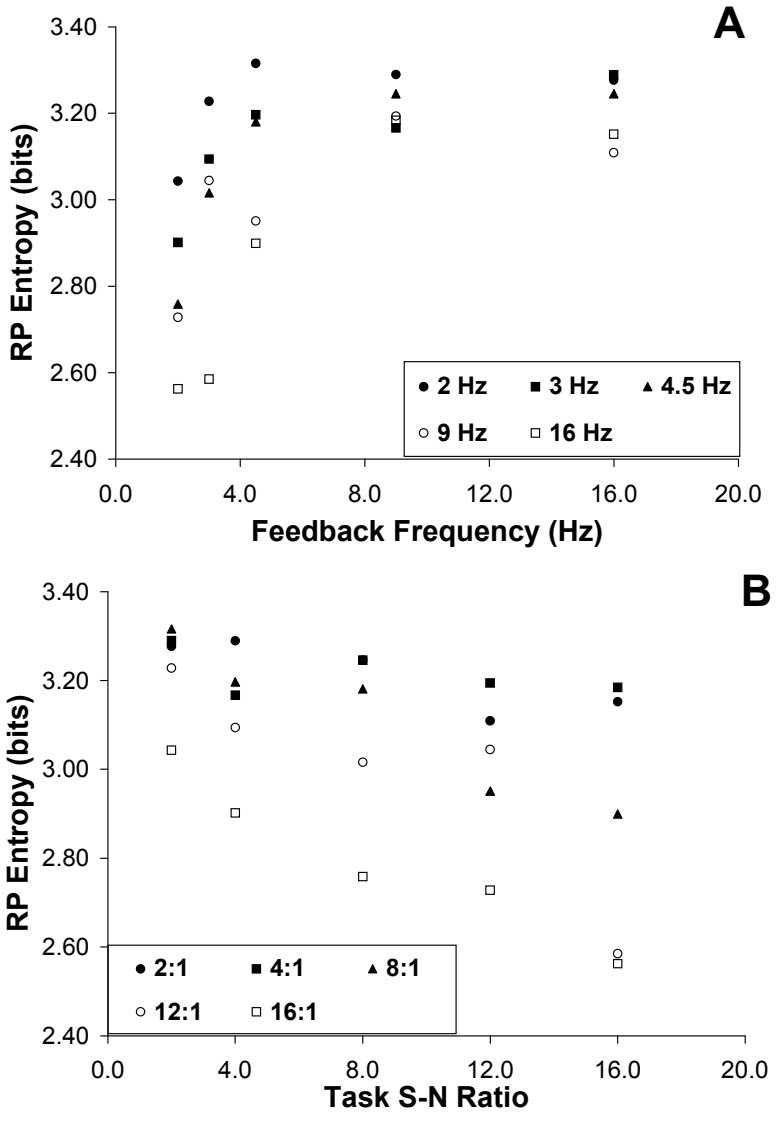

Figure 5.4. Effects of feedback frequency on relative phase (RP) entropy under different task constraints (A). Effect of task constraint at different feedback frequencies (B).

Figure 5.5 shows the relative phase entropy values fitted as functions of the task and environmental entropy and the parameter values of the fitted functions are presented in Table 5.1. The upper panel (Figure 5.5.A) presents the average effect of the environment on conditional relative phase entropy while the lower panel (Figure 5.5.B) illustrates the average effect of the task.

Table 5.1. Parameter values for relative phase entropy fitted as a quadratic function of environmental and task entropy.

	k	*A*
Environment	3.20	0.0186
Task	3.24	0.0277

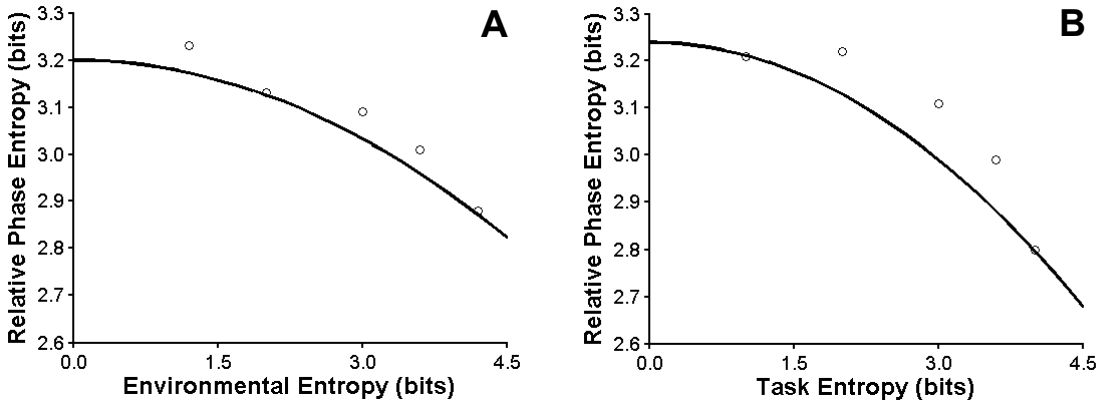

Figure 5.5. Effects of feedback frequency and task constraint represented as environmental (A) and task (B) entropies. The best fitting functions and r^2 values are also provided (Note: H_{env} = environmental entropy; H_{task} = task entropy).

The r^2-values for the environment and task were 0.90 and 0.73, respectively. From each of these fits, the average intercept and each of the coefficients applied to obtain the surface are presented in Figure 5.6. This surface is correlated to the data with an r^2-value of 0.73. Figure 5.6 provides a visual representation of the compensatory

nature of the task and environmental entropies on relative phase entropy. From this figure, it can be seen that the effects of a high task entropy (5.0 bits) and a low environmental entropy (0.0 bits) lead to an approximately similar relative phase entropy value as a low task entropy (0.0 bits) and a high environmental entropy (5.0 bits).

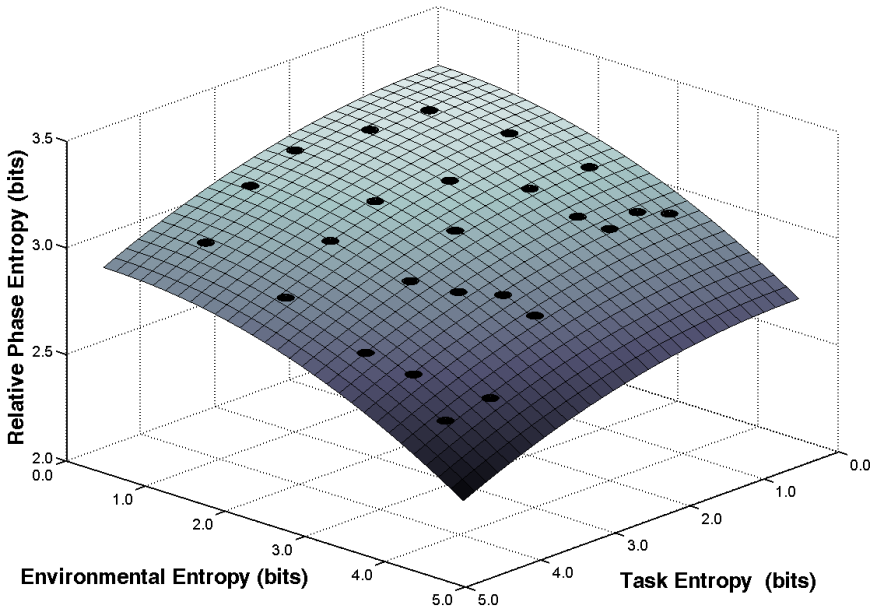

Figure 5.6. Quadratic surface generated from the coefficients obtained from the regressions presented in Figure 5.5. This surface is correlated to the data with an r^2 value of 0.73.

5.5. Discussion

The results of this study demonstrate compensatory tradeoffs in entropy between task, environment, and organism. The effect of the task constraint on the mean force produced was significant while both task and environmental effects on RMSE were significant. Entropy in the coordination pattern was significantly affected by both task and environmental entropy in a nonlinear relation. The data support the hypothesis of

compensatory effects of the environmental and task entropies on the entropy of the coordinated motor output.

5.5.1. Distributional Properties of the Total Force Output

The participants' tracking of the target force was enhanced with increased frequency of visual feedback (Slifkin et al., 2000; Sosnoff & Newell, 2005b), as marked significant but nonlinear decrease in RMSE with increasing feedback frequency. This finding shows that performance on the task is improved with the availability of more information from the environment, providing evidence for the efficacy of the experimental manipulations. RMSE was also reduced with increased task constraint, as the narrower bands reduced the magnitude of error.

The effects of feedback frequency on RMSE are in line with previous findings on isometric force production (Slifkin et al., 2000; Sosnoff & Newell, 2005b) and also those from tasks such as catching (Elliott, Zuberec, & Milgram, 1994) and precision walking (Assaiante, Marchand, & Amblard, 1989; Robertson, Collins, Elliott, & Starkes, 1994). In the latter studies, the number of discrete errors is reduced as feedback frequency is increased, be it foot placement or catching accuracy. Thus, greater feedback frequency is facilitative of error correction so that in our isometric force task, participants remain closer to the target force.

RMSE was reduced significantly when the error tolerance bands were narrowed. The post-hoc test of the Task main effect revealed a significant difference between the extreme conditions of the task, namely ratios of 2:1 and 16:1 while a second significant post-hoc difference was found the middle task constraint ratio of 8:1 and the task

constraint ratio of 16:1. Thus, the findings show that narrowing the width of the error tolerance bands results in a decrease in RMSE, and that the participants were complying with the accuracy demands of the task conditions.

5.5.2. Entropy in the Coordination of Force Output

The significant effects of the task and environment on the entropy of relative phase support the idea that increases in entropy at the level of the task and environment result in compensatory decreases in entropy at the level of the organism. The quadratic surface of Figure 5.6 captures a majority of the structure in the data and demonstrates that the effects of the task and environment were compensatory. This surface shows that the entropy in the coordination pattern can be preserved with an increase in task entropy and still allow for the movement goal to be achieved, but only if a decrease in environmental entropy of a similar magnitude occurs. In the event of an increase in environmental entropy, the entropy in the coordination pattern can be maintained with a decrease in task entropy of a similar magnitude.

The significant Task × Environment interaction, however, reveals an asymmetry on the quadratic surface (see Figure 5.6), and this is evidenced in the difference in the parameters of the surface obtained from the nonlinear regressions. From the regressions (Figure 5.5), the relative phase entropy was more accurately represented as a function of environmental entropy when compared to that of the task, as the r^2-values were 0.90 and 0.73 for environment and task, respectively. This shows that the relation between organismic and task entropy predicted by the quadratic function was not as good as the prediction of the relation between organismic and environmental entropy.

In tasks where the error tolerance was greater the participants were able to loosen the constraints upon the motor system, as reflected by more evenly distributed relative phase values, as greater variability in the coordination of force patterns are employed as solutions to the motor problem. Similarly, as the entropy of the environment was reduced, the relative phase values became more evenly distributed. The compensatory nature of the task and environmental entropies on the probability distribution of relative phase provides evidence that tasks with reduced error tolerance can still be performed with the same distribution of coordination patterns if more environmental information is provided and *vice versa*. Entropy conservation could provide a framework in which the task difficulty or environmental information can be adapted in order to alter the distribution of the fluctuations in the coordination pattern employed by the performers.

The representation of motor adaptation to different task and environmental contexts as a conservative process is in line with previous hypotheses that the magnitude of variance in human action is decreased with increased accuracy demands (Harris & Wolpert, 1998), as long as the assumption of a Gaussian distribution is upheld. Our current study, however, shows that the shape of the distribution of motor variance is systematically altered under different task and environmental contexts (see also Newell & Corcos, 1993; Newell, Deutsch, Sosnoff, & Mayer-Kress, 2005). Thus, the distribution of relative phase values becomes narrowed and peaked when the error tolerance of the task is narrowed and the entropy of the environment increases. The conservation law interpretation of motor adaptation also raises the possibility that the speed-accuracy tradeoff in human action is a reflection of a tradeoff between the entropies of the organism and task. In such a case, the increased demand on accuracy reduces the

probability of the achievement of the movement goal, and thus, an increase in task entropy. And, in cases where the individual is unable to perform the movement with a sufficiently low level of entropy (e.g., due to disability or disorder), the entropy of the task that would allow for the goal to be achieved would be decreased.

Overall, the results of this study are supportive of the idea of the compensatory nature of the effects of entropy of the task and environment on the entropy of the coordination of muscle forces. This is consistent with the postulation that human action is guided primarily by natural law (Kugler & Turvey, 1987). Within the dynamical systems framework, a narrowing of the probability distribution of relative phase represents an increase in coupling strength between the moving effectors (cf. Schöner et al., 1986; Turvey & Carello, 1996). Our findings also demonstrate that human action can be adapted to different task and environmental contexts through changes in coupling between the effectors involved in the task.

Chapter 6

General Discussion

The goal of this dissertation was to investigate the compensatory nature of the properties of the task, environment, and organism in human action. Chapter 3 of this dissertation examined the compensatory effects of the spatial and temporal entropies of the environment on the control of isometric force. Chapters 4 and 5 of the dissertation focus on the interaction of the task, organismic, and environmental constraints in motor adaptation. The dissertation seeks to characterize the process of motor adaptation as one of entropy conservation, as reflected in the compensatory effects of the task and environmental entropies on the force dynamics. The findings of this study provide preliminary evidence for conserved quantities in human action (Shaw & Turvey, 1999) and the potential for entropy as a conserved quantity.

6.1. Major Findings and Conclusions

6.1.1. Compensatory Properties of Visual Information

In general, greater frequency of visual feedback has been shown to possess the potential to increase the entropy in isometric force output (Slifkin et al. 2000; Sosnoff & Newell, 2005a,b) as well as reduce the occurrence of errors in tasks such as precision walking (Assaiante, Marchand, & Amblard, 1989; Robertson, Collins, Elliott, & Starkes, 1994) and ball catching (Elliott, Zuberec, & Milgram, 1994). Similarly, the effects of increased gain or spatial precision of visual feedback (up to a critical level) improves motor performance (Stephens & Taylor, 1974; Newell & McDonald, 1994; Beuter,

Haverkamp, Glass, & Carriere, 1995). However, the combined effects of spatial and temporal changes in feedback on motor performance have not yet been investigated.

Based on the findings of compensatory effects of velocity and contrast on the neural spike rate in the blowfly (de Ruyter van Steveninck et al., 1996), it was hypothesized that the spatial and temporal properties of visual feedback would have a similarly compensatory effect on the dynamics of isometric force. Thus, it was predicted, that increasing both gain and feedback frequency would result in increases in ApEn (Approximate Entropy - Pincus, 1991) of the isometric force time-series. Following from de Ruyter van Steveninck et al. (1996), the ApEn values would be represented as the elevation of a quadratic surface with feedback frequency and gain on the horizontal axes.

Gain and feedback frequency, however, are not in similar units, and thus, a uniform metric was necessary in order to allow the compensatory nature of visual feedback to be represented as a single process. As such, the various levels of gain and feedback frequency were converted into spatial and temporal entropy values, respectively. Spatial entropy was estimated based on the logarithm of the ratio of the pixel-to-Newton value to that of the screen height. Temporal entropy was estimated as the logarithm ratio of the feedback frequency to the Flicker-Fusion Threshold (Landis, 1954). The results showed that ApEn of the force output decreased nonlinearly as spatial and temporal entropy were increased.

These show that the irregularity or sequential entropy of an isometric force time-series are affected by the properties of the visual feedback. One could consider these results as a tradeoff between the entropy of the environment and the entropy of the action. Thus, as the environment becomes less predictable (i.e., provides less information) the

dynamics of the motor output become more predictable. However, the more interesting finding arising from the quadratic surface is that the effects of the spatial and temporal entropies of the environment are compensatory, as high levels of spatial entropy coupled with low temporal entropy and vice versa result in similar ApEn values. In the most simplistic sense, spatially precise feedback provided infrequently results in force output dynamics (characterized by ApEn) that are similar to situations when spatially imprecise feedback is provided at greater frequency.

In conclusion, the results of Experiment 1 present a view of the changes in force output dynamics with the properties of the environment as being one of an entropy tradeoff between the motor output and the environment. As the environmental entropy is increased, the entropy of the motor output is decreased and vice versa. The findings of Experiment 1 show that the spatial and temporal entropies of the environment have compensatory effects on the entropy of the force output.

6.1.2. Motor Adaptation as a Process of Entropy Conservation

Human action has been proposed as being the product of organismic, task, and environmental constraints (Newell, 1986). To date, there has yet to be an empirical determination of the confluence of the three categories of constraint in a single experiment using a process of entropy conservation as a unifying framework. One problem faced in the development of such experiments is the lack of a common metric to describe the various constraints on human action. From Shaw and Turvey (1999), the idea that human action is a process that involves conserved quantities. Such conserved quantities, are distributed across the dimensions of the action through compensatory

processes. In Experiment 1, the compensation between organismic and the environmental entropy was found, and potentially, a similar tradeoff between the task and organism is possible. From a convergence of the ideas presented in Newell (1986) and Shaw and Turvey (1999), it was hypothesized that human motor adaptation to different task and environmental contexts could be represented as the conservation of entropy.

Experiments 2 and 3 investigated this hypothesis using the isometric force control paradigm similar to Experiment 1. The entropy of the task was introduced into these experiments as a signal-to-noise ratio of the target force level and error tolerance. The entropy of the environment was estimated using the measure of temporal entropy employed in Experiment 1, with the logarithm of the ratio of feedback frequency to the Flicker Fusion Threshold. It was hypothesized that tradeoffs in entropy between the motor output and task, as well as the motor output and environment would occur. Furthermore, the effects of the task and environmental entropy on the motor output would be compensatory. Experiment 2 employed a unimanual task, and thus, the entropy at the level of the organism (i.e., the motor output) was measured using ApEn that was made conditional to the probability of the participants remaining within the error tolerance bands. Experiment 3 employed a bimanual isometric force, where participants were required to maintain the total force, and the entropy at the level of the organism was measured using the information entropy of the relative phase of the two finger forces. Similar to Experiment 2, the relative phase entropy was made conditional upon the total force remaining within the error tolerance bands.

In both Experiments 2 and 3, the entropy of the motor output decreased nonlinearly with increasing task and environmental entropy. The compensatory effects of

the task and environment on the organism were represented by the quadratic surface, where a similar organismic entropy values are predicted when a high task entropy is coupled with a low environmental entropy and vice versa. When both task and environmental entropy are at their highest, the entropy at the organism is at its lowest. Pairing the lowest task and environmental entropy levels resulted in the highest level of entropy in the motor output. These findings provide support for the conservation of entropy in human motor adaptation as the 3 entropies sum to a constant value, a scenario similar to that of the conservation of energy.

6.1.3. Coordinative Structures as Dissipative Structures

Kugler, Kelso, and Turvey (1980) raised the possibility that the coordinative structures or units of human action were open systems that dissipate energy and move toward an equilibrium state. As such, the motor system is viewed as a "self-optimizing" system (see Kugler & Turvey, 1987), that possesses resonant behavior at which the coordination patterns are most stable. These changes in stability and instability are products of a change in a linear control parameter that results in qualitative changes in the behavior of the system (Haken et al., 1985; Kugler et al., 1980). In the case of the HKB (Haken et al., 1985) model, the qualitative changes in behavioral dynamics, namely, the relative phase between the oscillating limbs are brought about by a continued increase in the oscillation frequency of the rhythmic movement. However, what has remained in question is how such control parameters are to be identified. This is especially difficult when the action is performed without a parameter that is both experimenter-defined and is being scaled continuously throughout the trial with no clearly observable qualitative

changes in the motor dynamics. Moreover, the HKB paradigm does not restrict the oscillation amplitudes and does not define explicit goals other than producing the desired coordination pattern specified by the experimenter. In Chapter 5, changes in the entropy of the coordination of the two fingers producing a total force were altered systematically with the entropies of the task and environment, resembling a conservative process. These changes in coordination dynamics occurred without any explicit instruction or restriction on a desired pattern, and thus, raising questions with regards to the view of coordinative structures as dissipative structures presented in Kugler et al. (1980).

Haken (2000) raised the point that systems should not be viewed exclusively as either open or closed, but rather should leave open the possibility that systems may be embedded within another. In this sense, a system studied at one level of analysis may reflect an open system that is embedded within a closed system at a higher or more macroscopic level of analysis and vice versa. In this dissertation, the conservation of entropy leads to the proposition that the human motor system is an open system, embedded within the closed system of human action. This view not only falls within the original theorizing of Kugler et al. (1980), but also extends this interpretation that movement dynamics are a part of a greater whole that is the task-organism-environment interaction.

6.2. Implications

The findings of the compensatory nature of the entropies in human action are consistent with the view that human action is guided by natural law (cf. Kugler & Turvey, 1987). From a less ambitious viewpoint, this dissertation presents human action

as a process of entropy compensation, for which movements performed in unpredictable environments lead to more predictable movements. Similarly, tasks that have a low relative error tolerance, that is, possessing higher indices of difficulty (in the terminology employed by Fitts, 1954) will also result in predictable actions. Beyond this, the compensatory nature of effects of task and environmental entropy point to the possibility that the predictability in the movement can be altered by providing more information from the environment to the performer, and vice versa. As such, changes in entropy at the level of the organism due to intention, development and aging, or practice and learning, will alter the level of task and environmental entropies that allow for the goal to continue to be achieved. Entropy conservation, as presented here, provides a simplistic view of motor adaptation that is based on the probabilistic properties of the movement patterns, task demands, and the environment.

From an empirical standpoint, this framework provides an avenue for comparing results across different experimental paradigms by accounting for differences in task and environmental contexts. In this sense, task-dependent differences in the results of studies employing different experimental paradigms can be understood and reconciled. It would be possible that converging conclusions may arise once the differences in task demands and feedback conditions across experiments placed within the construct of entropy conservation.

This conceptual framework also has implications for the field of human factors, where the information or feedback from the environment provided to the worker is increased in order to compensate for the greater difficulty in the task. The worker would benefit from this, as he/she will be able to employ a more broadly distributed range of

movement patterns in order to achieve the movement goal. Similarly, in work contexts where the environment is unpredictable, and cannot be altered, the task could be simplified, either by increasing the error tolerance, or reducing the task demands (e.g., amplitude or velocity). In this case, the worker would again receive the benefit of being able to employ a more varied range of movement patterns to complete the task. The potential for this area could be to reduce the load placed on the worker by creating situations in which the greatest number of movement patterns are able to achieve the goal.

This study also has the potential to influence the fields of aging and movement rehabilitation. Studies examining the loss of complexity in aging hypothesis (Lipsitz & Goldberger, 1992) have demonstrated that the fluctuations of a large set of physiological and motor processes possess more predictable sequences in the elderly. Lipsitz (2002) proposed that such increases in predictability in the physiological and motor dynamics are markers of frailty in the elderly. The conceptual framework and empirical findings in this dissertation, however, support the idea that greater predictability (or less complexity) in motor output should not necessarily be directly equated to poor performance (Newell & Vaillancourt, 2001) or ill-health (Vaillancourt & Newell, 2002). Rather, further evidence has been provided here, showing that the entropy of the motor output is context-dependent, and is primarily a reflection of the properties of the task and environment as well.

6.3. Limitations and Future Directions

One of the primary limitations of this dissertation is that the process of entropy conservation need not necessarily be restricted to the sum of quadratic functions used here. As this function was selected based on prior concepts and empirical findings, there is a possibility that other functions may be found under different movement contexts outside of isometric force production. Beyond this, the estimation of task and environmental entropy using a relative precision demand (similar to Fitts, 1954) and the Flicker-Fusion Threshold (Landis, 1954), respectively, will not generalize to all motor tasks. Novel means of estimating the entropy of the task and environment is necessary under different contexts, especially those where environmental feedback is not essential to the completion of the task, and changes independently of the behavior of the organism.

In the first part of this dissertation, asymmetries between the effects of spatial and temporal entropy in the environment on the force dynamics were found. One limitation in this work is that the estimation of spatial entropy is determined by the physical limitations of the computer monitor while the calculations of temporal entropy are bounded by the human visual system. Necessary for the future is to employ a larger feedback display that allows for the spatial limits of the visual system to be tested. One could then anchor the probability calculation for spatial entropy to the physiological limits of the human visual system. A second limitation is that the spatial entropy of the environment was not independent of the participants' actions. Future research in this area should involve objects or events within the environment that are independent of the actor's behavior. Systematically altering the spatial and temporal properties of these objects and events would further investigate the hypothesis that the effects of spatial and

temporal entropies of the environment have compensatory effects on the entropy of the motor output.

Although the second and third parts of this study provide preliminary evidence for entropy as a conserved quantity in human action, this dissertation has not yet involved the analysis of dynamic tasks and environments. Potentially, the error tolerance in a given task may change as the movement evolves over time. In addition, the movement of objects and the occurrence of events in the environment could also change as the action is performed. An example of such a situation would be actions performed within the context of a sport such as soccer, where the movements of the player and that of his/her teammates and opponents will evolve with the player's actions. Virtual reality based studies are necessary in this area, as virtual reality permits experimental manipulations of the environment that can be controlled and made similar across participants. Also, virtual reality based experimental paradigms would allow the environment to change dynamically with the movement itself, and greatly enhance our understanding of human action in evolving environments and movements with task error tolerances that are altered during the course of the movement.

A final limitation of this study deals with the idealized case of human movement, for which no errors are committed, and the goal is always achieved. In this study, the occurrence of errors in the task was accounted for through the use of conditional entropies. This correction was performed using the probability of remaining within the boundaries placed on the participant by the error tolerance bands. However, what remains in question at this point is the manner in which errors in action occur, and more importantly, the structure of the motor output leading up to the error. Beyond this, the

manner in which the process of entropy conservation becomes violated remains unknown. Similar to the conservation of energy and momentum, sources of dissipation are present in human action, just as with the examples of friction and restitution. Future studies could potentially locate sources where entropy is lost during human action.

"*To change with change is the changeless state.*"

-- Bruce Lee

Bibliography

Arutyunyan, G., Gurfinkel, G., & Mirskii, M. (1969). Organization of movements on execution by man of an exact postural task. *Biophysics, 14,* 1162-1167.

Assaiante, C., Marchand, A.R., & Amblard, B. (1989). Discrete visual samples may control locomotor equilibrium and foot positioning in man. *Journal of Motor Behavior, 21,* 72-91.

Beltrami, E. (1999). *What is random?* New York: Springer-Verlag.

Bernstein, N. (1967). *The coordination and regulation of movements.* Oxford: Pergamon.

Beuter, A., Haverkamp, H., Glass, L., & Carriere, L. (1995). Effect of manipulating visual feedback parameters on eye and finger movements. *International Journal of Neuroscience, 83,* 281-294.

Bracewell, R.M., Wing, A.M., Soper, H.M., & Clark, K.G. (2003). Predictive and reactive coordination of grip and load forces in bimanual lifting in man. *European Journal of Neuroscience, 18,* 2396-2402.

Carlton, L.G. (1992). Visual processing time and the control of movement. In L. Proteau & D. Elliott (Eds.), *Vision and motor control (pp. 3-31).* Amsterdam: Elsevier Science Publishers.

Cusumano, J.P., & Cesari, P. (2006). Body-goal variability mapping in an aiming task. *Biological Cybernetics, 94,* 367-379.

de Ruyter van Steveninck, R., Bialek, W., Potters, M., Carlson, R.H., & Lewen, G.D. (1996). Adaptive movement computation by the blowfly visual system. In D.L. Waltz (Ed.), *Natural and artificial parallel computation: Proceedings of the fifth NEC research symposium (pp. 21-41).* Philadelphia: SIAM.

Desmurget, M., & Grafton, S. (2000). Forward modeling allows feedback control for fast reaching movements. *Trends in Cognitive Sciences, 4,* 423-431.

Elliott, D. (1990). Intermittent visual pickup and goal directed movement: A review. *Human Movement Science, 9,* 531-548.

Elliott, D., Zuberec, S., & Milgram, P. (1994). The effects of periodic visual occlusion on ball catching. *Journal of Motor Behavior, 26,* 113-122.

Fitts, P.M. (1954). The information capacity of the human motor system in controlling the amplitude of movement. *Journal of Experimental Psychology, 22,* 1299-1313.

Fitts, P.M., & Peterson, J.R. (1964). Information capacity of discrete motor responses. *Journal of Experimental Psychology, 67,* 103-112.

Greene, P.H. (1969). Seeking mathematical models for skilled actions. In D. Bootzin and H.C. Muffley (Eds.), *Biomechanics (Proceedings of the First Rock Island Arsenal Biomechanics Symposium).* New York: Plenum Press.

Haken, H. (2000). *Information and self-organization: A macroscopic approach to complex systems.* Berlin: Springer.

Haken, H., Kelso, J.A.S., & Bunz, H. (1985). A theoretical model of phase transitions in human hand movements. *Biological Cybernetics, 51,* 347-56.

Hancock, P.A., & Newell, K.M. (1985). The movement speed accuracy relationship in spacetime. In H. Heuer, U. Kleinbeck, & K.H. Schmidt (Eds.), *Motor behavior: Programming, control, and acquisition (pp. 153-158).* Berlin: Springer-Verlag.

Harris, C.M., & Wolpert, D.M. (1998). Signal-dependent noise determines motor planning. *Nature, 394,* 780-784.

Hick, W.E. (1952). On the rate of gain of information. *Quarterly Journal of Experimental Psychology, 4,* 11-26.

Hyman, R. (1953). Stimulus information as a determinant of reaction time. *Journal of Experimental Psychology, 45,* 188-196.

Jagacinski, R.J., & Flach, J.M. (2003). *Control theory for humans.* Mahwah, NJ: Lawrence Erlbaum Associates.

Kantowitz, B.H., & Elvers, G.C. (1988). Fitts' law with an isometric controller: Effects of order of control and control-display gain. *Journal of Motor Behavior, 20,* 53-66.

Kugler, P.N., & Turvey, M.T. (1987). *Information, natural law, and the self-assembly of rhythmic movement: Theoretical and experimental investigations.* Hillsdale, NJ: Erlbaum.

Kugler, P.N., Kelso, J.A.S., & Turvey, M.T. (1980). On the concept of coordinative structures as dissipative structures: I. Theoretical lines of convergence. In G.E. Stelmach & J. Reqiun (Eds.), *Tutorials in motor behavior (pp. 1-49).* New York: North–Holland.

Lacquaniti, F., Terzuolo, C. & Viviani, P. (1983). The law relating the kinematic and figural aspects of drawing movements. *Acta Psychologica, 54,* 115-130.

Landis, C. (1954). Determinants of the critical flicker-fusion threshold. *Physiological Review, 34,* 259-286.

Lipsitz, L.A. & Goldberger, A.L. (1992). Loss of complexity and aging: potential applications of fractals and chaos theory to senescence. *Journal of the American Medical Association, 267,* 1806-1809.

Lipsitz, L.A. (2002). Dynamics of stability: The physiologic basis of functional health and frailty. *Journals of Gerontology Series A: Biological Sciences and Medical Sciences, 57,* 115-125.

Miall, R.C. (1996). Task-dependent changes in the visual feedback control: A frequency analysis of human manual tracking. *Journal of Motor Behavior, 28,* 125-135.

Newell, K. M., Liu, Y-T, & Mayer-Kress, G. (2005). Learning in the brain-computer interface: insights about degrees of freedom and degeneracy from a landscape model of motor learning. *Cognitive Processing, 6,* 37-47.

Newell, K.M. (1986). Constraints on the development of coordination. In M. Wade & H.T.A. Whiting (Eds.), *Motor development in children: aspects of coordination and control (pp. 341-360).* Dordrecht, Germany: Martinus Nijhoff.

Newell, K.M., & Corcos, D. M. (1993). Issues in variability and motor control. In K.M. Newell, & D.M. Corcos (Eds.), *Variability and motor control (pp. 1-12)*. Champaign, IL: Human Kinetics.

Newell, K.M., & McDonald, P.V. (1994). Information, coordination modes, and control in a prehensile force task. *Human Movement Science, 13,* 375-392.

Newell, K.M., & Slifkin, A.B. (1998). The nature of movement variability. In J.P. Piek (Ed.), *Motor behavior and human skill (pp. 143-160).* Champaign, IL: Human Kinetics.

Newell, K.M., Deutsch, K.M., Sosnoff, J.J., & Mayer-Kress, G. (2006). Motor output variability as noise: A default and erroneous proposition? In K. Davids, S. Bennett, & K. Newell (Eds.), *Variability in the movement system: A multi-disciplinary Perspective (pp. 3-22).* Champaign, IL: Human Kinetics.

Newell, K.M., Liu, Y-T, & Mayer-Kress, G. (2005). Learning in the brain-computer interface: insights about degrees of freedom and degeneracy from a landscape model of motor learning. *Cognitive Processing, 6,* 37-47.

Newell, K.M., & Vaillancourt, D.E. (2001). Dimensional change in motor learning. *Human Movement Science, 20,* 695-715.

Pincus, S.M. (1991). Approximate entropy (ApEn) as a complexity measure. *Proceedings of the National Academy of Science, 88,* 2297-2301.

Pincus, S.M., & Singer, B.H. (1996). Randomness and degrees of regularity. *Proceedings of the National Academy of Science, 93,* 2083-2088.

Robertson, S., Collins, J., Elliott, D., & Starkes, J. (1994). The influence of skill and intermittent vision on dynamic balance. *Journal of Motor Behavior, 26,* 333-339.

Schimdt, R.A., Zelaznik, H., Hawkins, B., Frank, J.S., & Quinn, J.T. (1979). Motor output variability – theory for the accuracy of rapid motor acts. *Psychological Review, 86,* 415-451.

Schöner, G., Haken, H., & Kelso, J.A.S. (1986). A stochastic theory of phase transitions in human hand movement. *Biological Cybernetics, 53,* 247-257.

Shannon, C.E. (1948). A mathematical theory of communication. *Bell System Technology Journal, 27,* 379-423.

Shannon, C.E., & Weaver, W. (1949). *The mathematical theory of communication.* New York: Wiley.

Shaw, R.E., & Turvey, M.T. (1999). Ecological foundations of cognition II. Degrees of freedom and conserved quantities in animal-environment systems. *Journal of Consciousness Studies, 6,* 111-123.

Shaw, R.S. (1984). *Dripping faucet as a model chaotic system.* Santa Cruz, CA: Aerial Press.

Sheridan, T.B. & Ferrell, W.R. (1974). *Man-machine-systems: Information, control, and decision models of human performance.* Cambridge, MA: MIT Press.

Slifkin, A.B., & Newell, K.M. (1999). Noise, information transmission, and force variability. *Journal of Experimental Psychology: Human Perception Performance, 25,* 837-851.

Slifkin, A.B., Vaillancourt, D.E., & Newell, K.M. (2000). Intermittency in the control of continuous force production. *Journal of Neurophysiology, 84,* 1708-1718.

Sosnoff, J.J., & Newell, K.M. (2005a). Intermittent visual feedback and the multiple time scales visual motor control of continuous force production. *Perception and Psychophysics, 67,* 335-344.

Sosnoff, J.J., & Newell, K.M. (2005b). Intermittency of visual information and the frequency of rhythmical force production. *Journal of Motor Behavior, 37,* 325-334.

Sosnoff, J.J., & Newell, K.M. (2006). Information processing limitations with aging in the scaling of isometric force. *Experimental Brain Research, 170,* 423-432.

Sosnoff, J.J., Jordan, K., & Newell, K.M. (2005). Information and force level interact in regulating force output during two and three digit grip configurations. *Experimental Brain Research, 167,* 76-85.

Stephens, J.A., & Taylor, A. (1974). The effect of visual feedback on physiological muscle tremor. *Electroencephalography and Clinical Neurophysiology, 36,* 457-464.

Turvey, M.T., & Carello, C. (1996). Dynamics of Bernstein's level of synergies. In M.L. Latash & M.T. Turvey (Eds.), *Dexterity and its development (pp. 339-376).* Mahwah, NJ: Lawrence Erlbaum.

Turvey, M.T., Fitch, H.L., & Tuller, B. (1982). The Bernstein perspective: 1. The problems of degrees of freedom and context-conditioned variability. In J.A.S. Kelso (Ed.), *Human motor behavior: An introduction (pp. 239–252).* Hillsdale, NJ: Lawrence Erlbaum.

Turvey, M.T., Shaw, R.E., & Mace, W. (1978). Issues in a theory of action: degrees of freedom, coordinative structures, and coalitions. In J. Requin (Ed.), *Attention and Performance VII, (pp. 557–598).* Hillsdale, NJ: Lawrence Erlbaum.

Vaillancourt, D.E., Haibach, P. S., & Newell, K.M. (2006). Visual angle is the critical variable mediating gain-related effects in manual control. *Experimental Brain Research, 173,* 742-750.

Vaillancourt, D.E., & Newell, K.M. (2002). Changing complexity in human behavior and physiology through aging and disease. *Neurobiology of Aging, 23,* 1-11.

Vaillancourt, D.E., & Russell, D.M. (2002). Temporal capacity of short-term visuomotor memory in continuous force production. *Experimental Brain Research, 145*, 275-285.

van Beers, R.J., Baraduc, P., & Wolpert, D.M. (2002). Role of entropy in sensorimotor control. *Philosophical Transactions of the Royal Society B: Biological Sciences, 357,* 1137-1145.

Warren, W.H. (2006). The dynamics of perception and action. *Psychological Review, 113,* 358-389.

Woodworth, R.S. (1899). The accuracy of voluntary movement. *Psychological Review, 3,* 1-119.

S. LEE HONG – VITA

I. Formal Education

A. Graduate Education

Ph.D. – The Pennsylvania State University, Kinesiology, 2007
Dissertation: "Entropy Compensation in Human Motor Adaptation"

M.S. – Ithaca College, Exercise Physiology, 2004
Thesis: "The Specificity of Learning Hypothesis: Effects of Altering Stimulus Conditions on Learning"

B. Undergraduate Education

B.S. – Liverpool John Moores University, Science and Football (Soccer), 2001

II. Refereed Scholarly Publications

A. Peer-Reviewed Journal Articles

Hong, S.L., & Newell, K.M. (2006). Practice effects on local and global dynamics of the ski-simulator task. Experimental Brain Research, 169, 350-360.

Hong, S.L., & Newell, K.M. (2006). Change in the organization of degrees of freedom with learning. Journal of Motor Behavior, 38, 88-100.

Hong, S.L., Bodfish, J.W., & Newell, K.M. (2006). Power-law scaling for macroscopic entropy and microscopic complexity: Evidence from human movement and posture. Chaos, 16, 013135.

Hong, S.L. (2007). The dynamics of structural and functional complexity across the lifespan. Nonlinear Dynamics in Psychology and Life Sciences, 11, 219-234.

Hong, S.L., Lee, M-H., & Newell, K.M. (2007). Magnitude and structure of force variability: Mechanical and neurophysiological influences. Motor Control, 11, 119-135.

Stratton, S.M., Liu, Y-T., Hong, S.L., Mayer-Kress, G., & Newell, K.M. (in press). Snoddy (1926) revisited: Time scales of motor learning. Journal of Motor Behavior.

Morrison, S.M., Hong, S.L., & Newell, K.M. (in press). Randomness and regularity in postural sway. Experimental Brain Research.